INVESTIGATION OF O-RING ADHESION IN SPACE MECHANISMS

A Major Qualifying Project Report

Submitted to the Faculty

of the

WORCESTER POLYTECHNIC INSTITUTE

In partial fulfillment of the requirements for the

Degree of Bachelor of Science

in Mechanical Engineering

By:

Tyler Albee

Katherine Mims

Date: 11 October 2012

Approved By:

Professor Nikolaos A. Gatsonis,Advisor

Mechanical Engineering Department, WPI

Jesse Mills, Affiliate Advisor

Carl Hart, Affiliate Advisor

Group 75, MIT Lincoln Laboratory

This work is sponsored by the Department of the Air Force under the United States Air Force contract number FA8721-05-C-002. The opinions, interpretations, recommendations, and conclusions are those of the author(s) and are not necessarily endorsed by the United States Government.

Abstract

The project involves the investigation of adhesion in O-rings used in a space communications mission designed by MIT Lincoln Laboratory. Experiments and testing were conducted with sixteen types of O-rings and twelve different mating interfaces. Test results are presented for adhesion force, thermal survival, adhesion at varying temperatures, outgassing, force vs. deflection, optical metrology and surface roughness, and residue analysis. Free body diagram analysis and finite element modeling are presented. The selection of an O-ring and interface that fits the design parameters for the mission are presented. This investigation advances the understanding of the adhesion process in O-rings used in deployable space mechanisms.

Acknowledgements

The project team would like to thank the following people who were greatly involved in helping us with this project:

WPI Staff:

- Professor Gatsonis – Project Advisor
- Professor Clancy – Site Coordinator
- Professor Iannacchione –WPI Professor

MIT Lincoln Laboratory Staff:

- Carl Hart – Supervisor, Group 71
- Jesse Mills – Supervisor, Group 75
- Todd Mower – Technical Staff, Group 75
- Sharon Hardiman – Secretary, Group 75
- Carol Mullinax – Secretary, Group 75
- Peter Anderson – Technician, Group 72
- Russ Goodman – Specialist, Group 81
- Scott Hillis – Clean Room Technician, Group 72
- Tasha Naylor – Clean Room Technician, Group 72
- Glenn Matot – Clean Room Technician, Group 72

Acronyms

CVCM: Collected Volatile Condensable Materials

DMA: Dynamic Mechanical Analyzer

FBD: Free Body Diagram

FEA: Finite Element Analysis

FEM: Finite Element Modeling

FEP: Fluorinated Ethylene Propylene

HOPA: High Output Paraffin Actuator

LL: Lincoln Laboratory

MQP: Major Qualifying Project

ST: Space Terminal

THF: Tetrahydrofuran

TML: Total Mass Loss

VB: Vacuum Baked

WPI: Worcester Polytechnic Institute

Any O-Ring or Surface Related Acronyms can be found in Table 1 and Table 2.

Graph Color References

O-Rings:	Surfaces:
O-Rings as Received - Green	Aluminum - Light Blue
FEP Encapsulated - Dark Blue	Invar - Red
Vacuum Baked - Black	HTR - Orange
Any other treatment - Tan	N615 - Purple

Table of Contents

Abstract ii
Acknowledgements iii
Acronyms iv
Graph Color References iv
Table of Figures 3
Table of Tables 4
Chapter 1: Introduction 5
1.1 Selecting O-Rings for the Space Terminal (ST) 7
1.2 Project Objectives and Approach 10
Chapter 2: Survival and Opening of the Launch Latch: Mechanical Analysis 13
2.1 Free Body Diagram Analysis 13
2.2 Finite Element Modeling of the Pawl Arm 17
Chapter 3: O-Ring Test Standards 20
3.1 O-Ring and Interface Test Subjects 20
3.2 O-Ring Sample Preparation 24
3.3 Dynamic Mechanical Analyzer Testing for Adhesion 27
3.4 Dynamic Mechanical Analyzer Testing at Hot and Cold Temperatures 31
3.5 Thermal Survival Testing 32
3.6 Stiffness Testing 33
3.7 Durometer Testing 33
3.8 Outgassing Testing 34
3.9 Optical Metrology and Surface Roughness 34
3.10 Residue/Squish Testing 35
Chapter 4: O-Ring and Interface Data Analysis and Results 36
4.1 Adhesion Analysis 36
4.2 Thermal Survival Testing Analysis 39
4.3 Stiffness and Durometer Analysis 41
4.4 Outgassing Results 44
4.5 Optical Metrology and Surface Roughness Results 45
4.6 Residue/Squish Test Results 49

4.7 DMA Temperature Testing Analysis 50
4.8 Overall O-Ring Testing Results 51
Chapter 5: Launch Latch Final Analysis and Component Selection 52
Chapter 6: Conclusions and Recommendations 54
6.1 Factors in O-Ring Adhesion 54
6.2 Factors in Interface Adhesion 56
6.3 Possibilities for Future Research 57
Work Cited: 59
Appendix A: DMA Testing Standards 60
Appendix B: Outgassing Standards 65
Appendix C: HOPA Data Sheet 66
Appendix D: Surface Coating Specifications 67
Appendix E: O-Ring Specification Sheets 73
Appendix F: Vlier Spring Specifications 83
Appendix G: CD Files and References 84

Table of Figures

Figure 1: Space Terminal with Launch Latch Annotated. 7
Figure 2: Latch Components Design Criteria to be Specified. 8
Figure 3: Latch Components to be Analyzed. 9
Figure 4: Forces and Moments Applied to the Launch Latch 10
Figure 5: Free Body Diagram of Launch Latch Door 13
Figure 6: Free Body Diagram of the Hugging Arm Assembly 14
Figure 7: Free Body Diagram Calculation for HOPA Force and Frankenstein Bolt Force 15
Figure 8: Forces Acting on the Latch Door during Opening 16
Figure 9: Adhesion Force vs. Forces Opening the Latch Door 17
Figure 10: Pawl Arm Modeling of Applied and Fixed Forces. 18
Figure 11: Stress Calculations Completed by SolidWorks SimulationXpress 20
Figure 12: O-Ring Testing Set-Up 25
Figure 13: O-Ring Bottom Plate with O-Rings and Washers 26
Figure 14: DMA Test as the Top Plate is Lifting 28
Figure 15: TA Analysis Software for Performing DMA Tests 29
Figure 16: Adhesion Data Retrieval in Universal Analysis 30
Figure 17: O-Ring Adhesion Measurement Spreadsheet Example 31
Figure 18: Adhesion of All O-Ring Types on Chemical film Aluminum 37
Figure 19: Adhesion of V0986 on All Interface Types 38
Figure 20: S0899 Adhesion for Different O-Ring Batches. 39
Figure 21: Thermal Survival Before and After Pictures of E1100 40
Figure 22: 3D Image of V0986 Before and After Thermal Testing 41
Figure 23: Force vs. Deflection Data for RTV566 42
Figure 24: Force Required to Compress O-Rings 43
Figure 25: O-Ring Stiffness vs. Durometer 43
Figure 26: Surface Roughness and Optical Metrology for Aluminum Based Interfaces 45
Figure 27: Surface Roughness and Optical Metrology of Invar Based Surfaces 46
Figure 28: Surface Roughness vs. Adhesion 47
Figure 29: O-Ring Results when Tested with Both HTR and CFM 48
Figure 30: O-Ring Results when Tested with Both N615 and CFM 49
Figure 31: Squish Test Residue Results 49
Figure 32: Residue vs. Adhesion Results 50
Figure 33: Adhesion vs. Temperature Results for Selected O-Rings 51
Figure 34: Overall Opening Force 52

Table of Tables

Table 1: Table of O-Ring Types and their Identifying Information 21
Table 2: Table of Interface Types and their Identifying Information 23
Table 3: O-Ring Outgassing Results..... 44

Chapter 1: Introduction

An O-ring is a torus, or doughnut shaped ring generally molded from an elastomer and are commonly used as a seal to prevent the loss of fluid or gas between two interfaces. However, O-ring seals can be used as the interface between mated components, as they form an effective contamination seal for optical instruments while also providing some form of damping through the viscoelastic property of the material. Most space flight optical systems for example feature mechanisms utilizing O-rings for contamination control that are deployed once the payload is in orbit. Some examples include motorized covers or doors for optical instruments along with restraint latches which protect hardware during launch conditions. There are many aspects to the selection of an O-ring and its mating interface, however one of the most important and least understood parameters is parasitic adhesion.

O-Ring adhesion is the result of an unknown interaction that occurs between the surface the O-ring presses against when forming a seal and the O-ring itself. The adhesion forces between the O-ring and its mating interface "lock" the two surfaces together. Depending on the amount of adhesion force, it can be difficult to separate the two surfaces. The magnitude of adhesion is not easily calculated or predicted due to its variability with temperature, O-ring chemical composition, mating surface material and finish, along with O-ring lubrication, if applicable, in addition to the unknown source of adhesion. Adhesion, if left unchecked, could potentially lead to the mechanism not separating once on orbit so great care must be taken in specifying an O-ring and its mating interface in a deployable contamination seal design. To address this concern of adhesion, O-rings can be coated with thin films of Teflon, lubricated, encapsulated in thicker wall Teflon tubing, or vacuum baked depending on the requirements of their use.

The Massachusetts Institute of Technology's Lincoln Laboratory (LL) had at one time experienced O-ring adhesion complications in an optical sensor system during thermal vacuum testing at cold conditions. After risk reduction testing and analysis, this particular program decided to eliminate O-ring adhesion altogether by removing the O-ring and replacing it with Vespel buttons. Currently, LL is preparing a new Optical Module (OM) including a Launch Latch that utilizes both labyrinth passages and an O-ring for contamination mitigation. To analytically show that the latch has appropriate margin against O-ring adhesion, measurements of O-ring adhesion were required. This was one of the major motivations for this MQP project.

The functioning of O-rings, particularly adhesion to their interfacing surfaces, can determine the success or failure of major projects, and predicting modes of failure can be difficult. Our understanding about the causes of O-ring adhesion is limited which makes the design of components or choice of O-rings to avoid adhesion somewhat arbitrary. Current published information (e.g. NASA) focuses on only a few O-rings that have known low outgassing properties and does not provide a complete dataset for designing to minimize adhesion between O-rings and adhering surfaces. Preferably, a relation between the chemical composition of O-rings, their interfacing materials and adhesion, or a guide to common O-rings and their adhesion when interfaced with a material would be the ideal situation.

The main goal of this MQP will be to investigate the underlying fundamental physics and mechanisms that cause and/or reduce adhesion between O-rings and their mating interfaces, to be used by a space terminal mission. The MQP will attempt to identify parameters that can lead to O-ring adhesion and determine from a fundamental perspective which of these parameters affect adhesion to the greatest extent with a goal being on reducing this parasitic force or even finding a zero adhesion solution.

1.1 Selecting O-Rings for the Space Terminal (ST)

The ST is part of a larger space communication system, which implements a latch that must open once on orbit. The ST uses an O-ring along with labyrinth passages to seal the Launch Latch as shown in Figure 1.

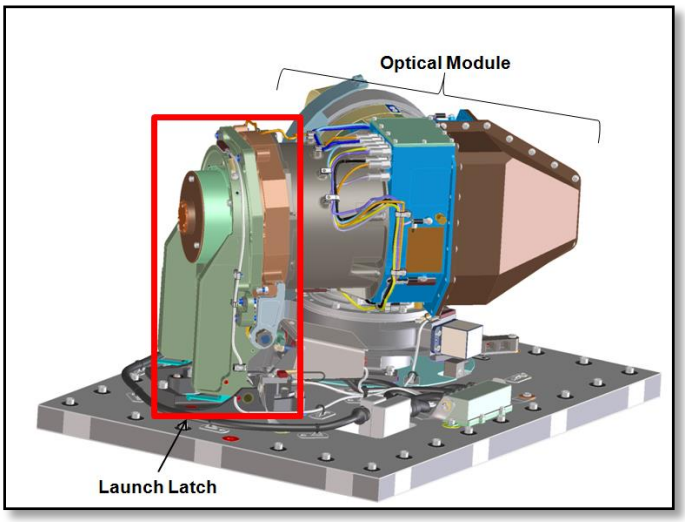

Figure 1: Space Terminal with Launch Latch Annotated.

The Launch Latch is designed to restrain the Optical Module during launch and all components must have positive margin against yielding. Once on orbit, the latch must be able to open under all worst case environmental loading conditions. Most of the forces that are involved in both launch and actuation are known or predictable, with the exception of the O-ring adhesion force. The objective of this MQP requires the proper selection of the O-ring used for the ST to ensure that the latch can adequately restrain the optical module during transport and launch and reliably open once on orbit. The design investigation also involves the selection of the O-ring mating interface material, the lower torsion springs of the latch, and the upper Vlier springs as shown in Figure 2. The upper Vlier springs provide first motion of the Launch Latch away from the

mating O-ring interface and the potential energy stored in the lower torsion springs are responsible for driving the Launch Latch away from the Optical Module.

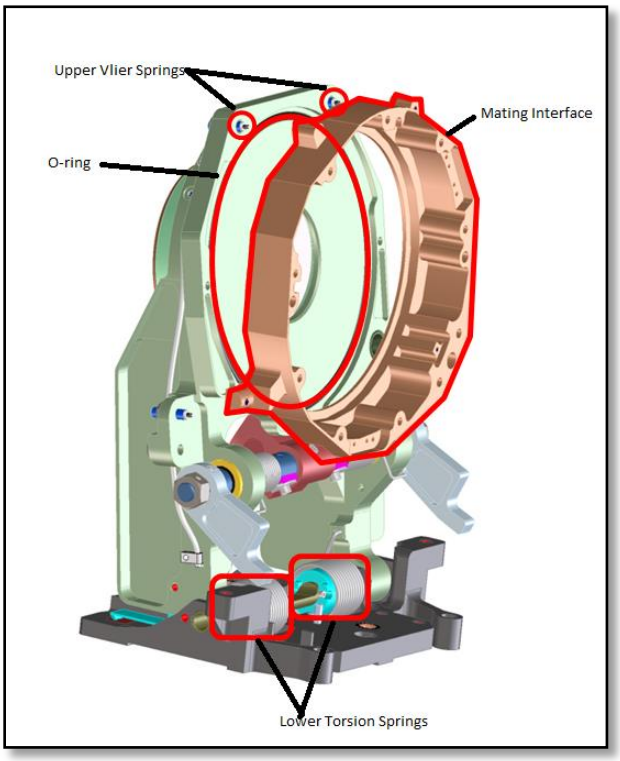

Figure 2: Latch Components Design Criteria to be Specified.

The opening of the latch greatly depends upon the functionality of the HOPAs (High Output Paraffin Actuators) and the Pawl Arm, as shown in Figure 3. The HOPAs act as a pin puller, holding the Launch Latch closed until the door is to be opened, and then releasing the door when required to. The HOPAs must not yield due to the force induced on them by holding the latch door closed, by applying force to the Pawl Arm. The Pawl Arm also must not break due to the applied forces acting on it during the survival and opening stages of the Launch Latch. The latch pin will be accounted for, as well as the friction it applies when opening the latch.

There are several specific design requirements, aside from survival and opening of the latch, which exist for the function of the latch and the ST telescope:

a.) The materials utilized, specifically the O-ring and its interfacing surface, must be low outgassing materials.

b.) A safety factor of 1.25 must be applied when analyzing for yield stress of identified components or O-ring adhesion.

c.) The load applied to the HOPAs by the Pawl Arm of the Launch Latch cannot exceed the max allowable shear force.

d.) The Pawl Arm must not exceed the max allowable yield stress of 120 ksi which includes a safety factor of 1.25.

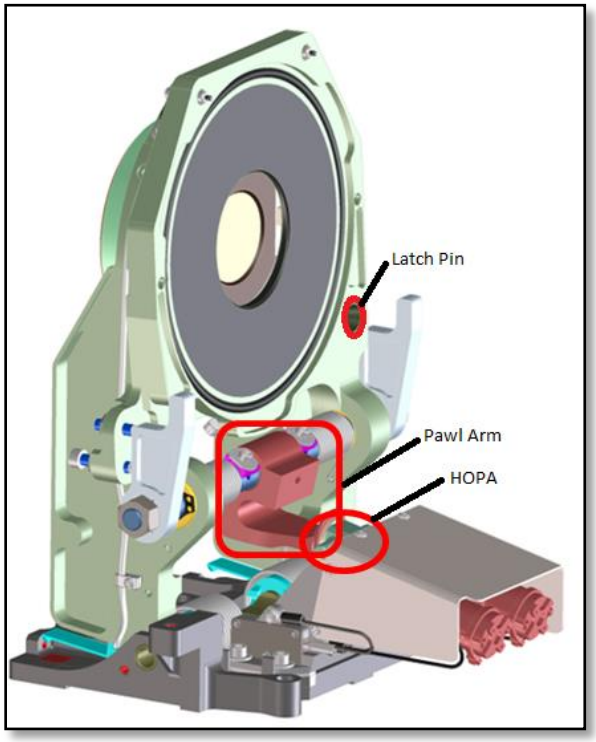

Figure 3: Latch Components to be Analyzed.

The selection of the lower torsion springs and upper viler springs is critical to overcoming the parasitic forces from the O-ring adhesion and latch pin friction to result in a successful opening stage. The O-ring has the largest amount of uncertainty associated with its adhesion force, and will be tested in various scenarios to decrease the amount of unpredictability associated with O-ring adhesion. The components must be selected for the Launch Latch design to ensure the survival of hardware and successful opening in orbit.

1.2 Project Objectives and Approach

The main objective of this project is to identify a low adhesion O-ring for the ST and evaluate its performance with the other components of the latch. Free-body diagrams will be generated using the information and notation shown in Figure 4. By evaluating the known force reactions (shown in green) and the O-ring test data, spring constants for the upper Vlier and lower torsion springs were chosen. With the spring and O-ring force calculated, the overall HOPA force to keep the latch closed was determined.

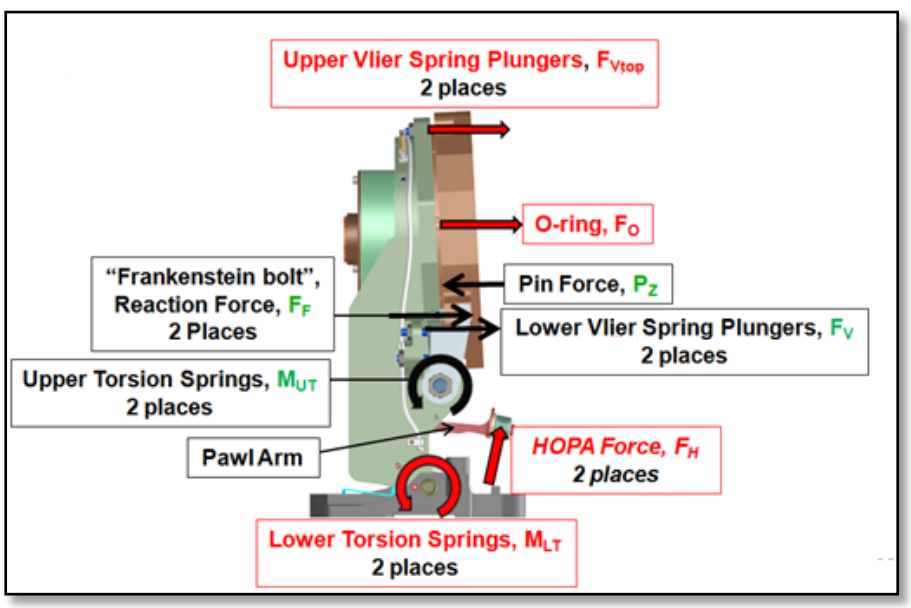

Figure 4: Forces and Moments Applied to the Launch Latch

Analysis using finite element modeling (FEM) based off the calculated HOPA force allowed the stress of the Pawl Arm to be computed. The yield point of the Pawl Arm and the maximum HOPA force was determined to ensure that the Optical Module was successfully held shut through the entry into space.

To investigate O-ring adhesion and fulfill the design requirements, several experimental approaches were taken to analyze the functioning of the ST Launch Latch, which are summarized below.

a) Perform Dynamic Mechanical Analyzer (DMA) testing to accurately measure the adhesion force between O-rings and their paired interfaces. A minimum of five trials of each of the 57 proposed sample types were conducted. During these tests, a number of O-rings were evaluated against a common surface to compare their overall adhesion to a common surface. Tests were conducted with particular O-rings with varying interfaces and treatments, such as vacuum baking or thin-film coatings, and compared to their non-treated counterparts.
b) Perform adhesion testing at various temperatures using the DMA furnace to develop an understanding of O-ring adhesion at cold and hot temperatures.
c) Perform thermal survival testing to observe the effects of extreme cold on O-ring survival.
d) Perform low outgassing testing through an outside vendor per ASTM 595-07 standards, which is further explained in the outgassing section.
e) Perform stiffness testing to evaluate the amount of force required to compress O-rings a particular distance. This data was then used to model the amount of force required to close the Launch Latch and compress the O-ring 0.010 inches to create a seal.

f) Obtain optical metrology and surface roughness measurements to investigate the relation between O-ring adhesion and the mating surfaces roughness.

g) Perform basic analyses involving free body diagrams to understand the force interactions of the Launch Latch and the effect of O-ring adhesion on the Launch Latch.

The analytical and experimental results were used to select viler plunger, lower torsion springs, an O-ring and its mating interface. The results of this MQP provide assurance for the successful operation of the ST Launch Latch.

Chapter 2: Survival and Opening of the Launch Latch: Mechanical Analysis

The Launch Latch was analyzed using free body diagrams to formulate equations that described the relation of forces and moments within the system. The required HOPA force was calculated and used to determine that the HOPA's would not fail. Finite element modeling (FEM) was completed for the Pawl Arm to ensure that it would not reach its yield stress during the survival or opening stages. This chapter describes the process and physical analysis of the Launch Latch and Pawl Arm in both the survival and opening stages.

2.1 Free Body Diagram Analysis

The Launch Latch door was reviewed for its force interactions when in the closed position, survival stage, as shown in Figure 5**.**

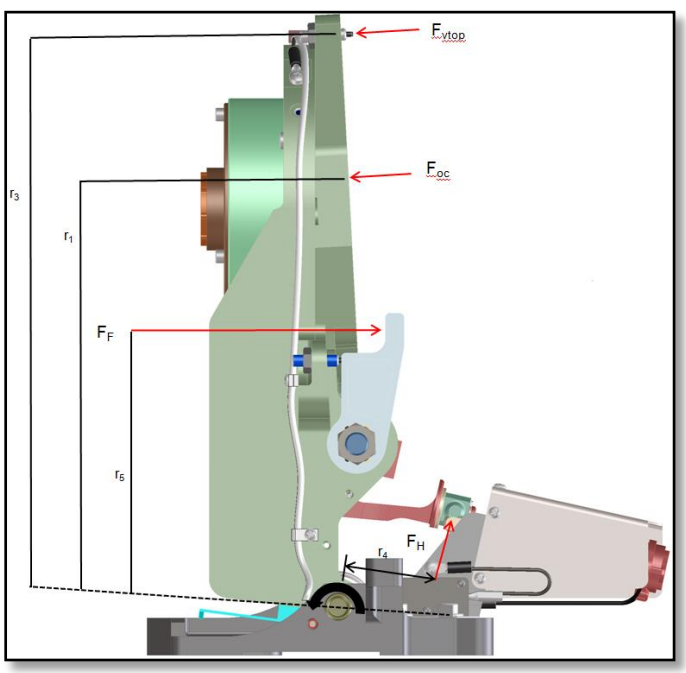

Figure 5: Free Body Diagram of Launch Latch Door

The main forces involved were; F_{vtop}: the force applied by the upper Vlier springs, F_{oc}: the force required to compress the O-ring, F_v: the force applied by the lower Vlier springs, F_F: the force applied by the Frankenstein bolt force (part of the Optical Module), F_H: the HOPA force, and M_{LT}: the moment applied by the lower torsion springs. The slight angle of the Launch Latch/Optical Module interface was 3°, and was found to be negligible regarding the magnitude of forces being predicted. The angle of the HOPA force, acting perpendicular to the end of the Pawl Arm, shown as theta, was 12.81°. The moment arms for the forces in all free body diagrams were determined using the SolidWorks CAD model. The sum of the moments about the lower axle resulted in two unknown forces, F_H and F_F. In order to solve for both forces, a secondary force relation equation was required. To find this second equation, the hugging arm assembly was reviewed and the moments about the hugging arm pin in the system calculated, as shown in Figure 6**.**

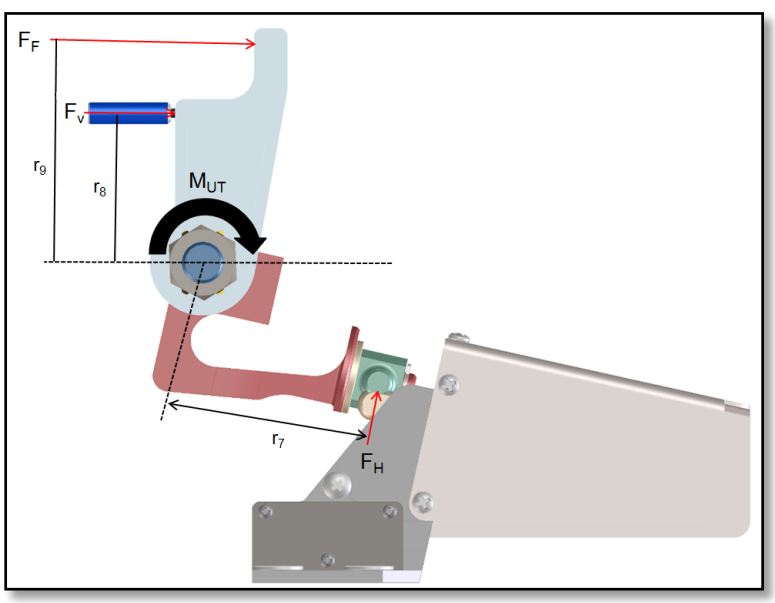

Figure 6: Free Body Diagram of the Hugging Arm Assembly

The HOPA force was calculated in relation to the O-ring forces, the upper Vlier springs and lower torsion springs. The lower Vlier springs were given as 2.3 lbf each and the upper torsion springs as 3 lbf-in each. The numerical values and equations for both states were input into a MathCAD file and evaluated to find the overall HOPA force and F_F, the Frankenstein bolt force, simultaneously, as shown in Figure 7. The HOPA force is the top result of inverse matrices calculation, and the Frankenstein bolt force is the lower result.

$F_{vtop} := 4.5lbf \quad F_{oc} := 27lbf \quad P_z := 5.6lbf \quad F_v := 2.3lbf$

$M_{LT} := 5in \cdot lbf \quad F_{adhesion} := 3.7lbf$

$r_1 := 5.394in \quad r_2 := 3.75in \quad r_3 := 7.7303in \quad r_4 := 1.26in$

$r_5 := 3.76in \quad r_7 := 1.503in \quad r_8 := 1.13in \quad r_9 := 1.53in \quad M_{UT} := 3lbf \cdot in$

Free Body Equations for the Latch: Sum of The Moments

$2F_{vtop} \cdot r_3 + F_{oc} \cdot r_1 + 2 \cdot F_H \cdot r_4 - 2F_f \cdot r_5 + 2M_{LT}$

Free Body Equations for the Hugging Arm Assembly: Sum of the Moments

$2F_H \cdot r_7 - 2 \cdot F_f \cdot r_9 - 2F_v \cdot r_8 - 2M_{UT}$

Matrix Evaluation:

$a := -2F_{vtop} \cdot r_3 - F_{oc} \cdot r_1 - 2.M_{LT} \quad b := 2F_v \cdot r_8 + 2.M_{UT}$

$$A := \begin{pmatrix} 2 \cdot r_4 & -2 \cdot r_5 \\ 2.r_7 & -2r_9 \end{pmatrix} \quad B := \begin{pmatrix} a \\ b \end{pmatrix}$$

$$A^{-1}B = \begin{pmatrix} 51.924 \\ 47.348 \end{pmatrix} lbf$$

Figure 7: Free Body Diagram Calculation for HOPA Force and Frankenstein Bolt Force

To evaluate whether the chosen O-ring were reasonable, the forces acting on the door just at the opening state were evaluated. The forces acting on the latch door just prior to opening are the upper Vlier springs and lower torsion springs, as well as $F_{adhesion}$: the adhesion force from the O-ring adhering to its mating surface and P_z: the force of the latch pin on the latch door as shown in Figure 8**.**

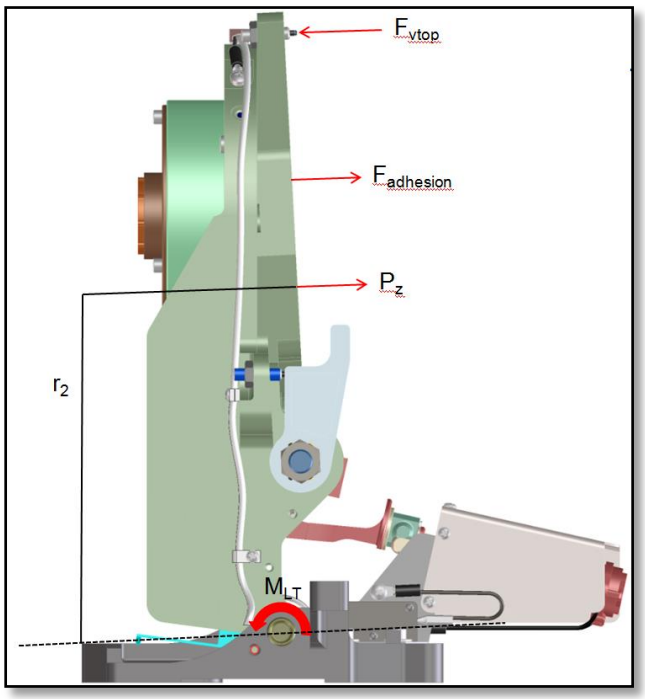

Figure 8: Forces Acting on the Latch Door during Opening

The adhesion force, determined by measurement, was applied to the equation for the latch opening with the upper Vlier and lower torsion springs to ensure the opening of the latch door. The pin force P_z, was given as 5.6 lbf in the problem statement, which resulted from frication at the pin/socket interface. As shown in Figure 9 below, if the forces of the lower torsion springs, upper Vlier springs and latch pin are greater than the O-ring adhesion force the latch will open.

$$F_{adhesion} = 3.7\,lbf$$

$$\frac{\left(2M_{LT} + 2F_{vtop}\cdot r_3 - P_z\cdot r_5\right)}{r_1} - F_{adhesion} = 2.849\cdot lbf$$

Figure 9: Adhesion Force vs. Forces Opening the Latch Door

The final O-ring and correlating HOPA force was then analyzed on an elemental level to make sure the stress and displacement of the Pawl Arm was within a reasonable range.

2.2 Finite Element Modeling of the Pawl Arm

Finite element modeling was conducted for the Pawl Arm. The required HOPA force determined by the free body diagram analysis results was then used to model the stress and displacement of the Pawl Arm. The modeling was completed using SolidWorks SimulationXpress. The Pawl Arm's attachment point to the Launch Latch window was modeled as a fixed point, annotated by the green arrows in Figure 10. The applied HOPA force required to hold the Launch Latch closed is shown in purple. The applied force is applied perpendicular to the Pawl Arm shaft.

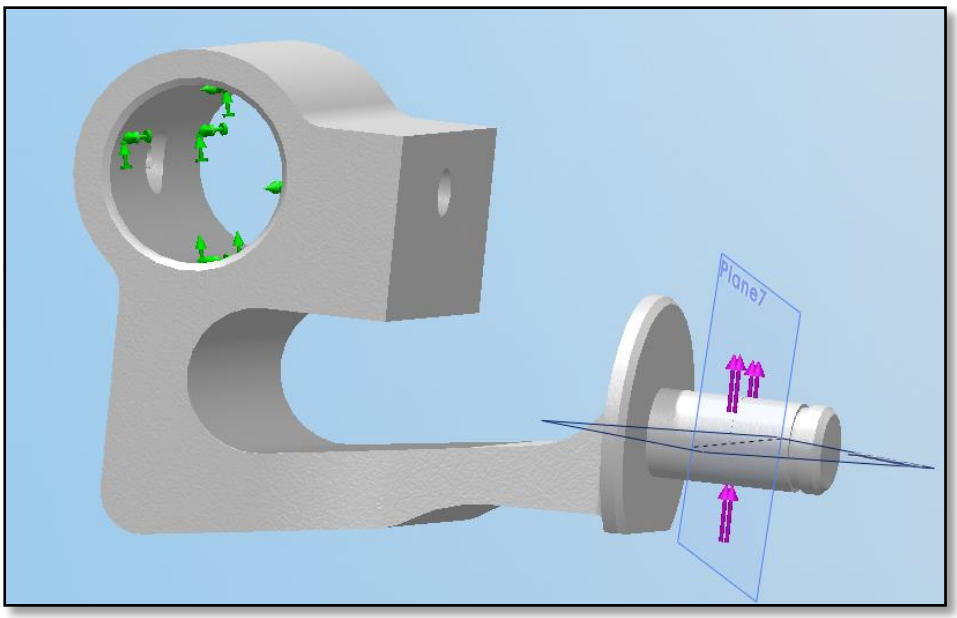

Figure 10: Pawl Arm Modeling of Applied and Fixed Forces.

The Pawl Arm is fabricated from beryllium copper (C17200, Alloy 25) HT temper certified per AMS 4535. The material has an elastic modulus of $19x10^6$ psi, a density of 0.302 lb/in^3, tensile yield strength of 150 ksi and an ultimate tensile strength of 175 ksi. These properties were entered into SolidWorks for the Pawl Arm component. The yield strength was divided by the safety factor of 1.25 to provide the maximum allowable yield stress of 120 ksi.

The adhesion force for a full O-ring was calculated based on the adhesion force per inch calculated for the final O-ring samples. The adhesion force was calculated on the upper bound of a 95% confidence interval, to account for a worst case scenario, and then multiplied by the safety factor of 1.25. The adhesion force for the full O-ring was then entered into the MathCAD calculation, along with the O-ring compression force and chosen upper Vlier spring and lower torsion spring values to calculate the HOPA force. In the problem statement provided, there are three load cases of which induce stress to the Pawl Arm. The first load case is the amount of force required to hold the Launch Latch window shut, which we are referring to in this report as

HOPA force, includes the O-ring compression force and other internal forces in the system. The other two load cases include the preload force and dynamic forces. Both these latter cases must be considered since they keep the O-ring compressed under worst case vibration loading. The preload force was given as 256 lbf and was predicted using FEA. The 3-sigma random vibration force of 53 lbf was given and reflects dynamic forces exerted on the HOPA's during launch. Together, the dynamic and preload forces add a total of 309 lbf to the Pawl Arm, before the additional force required to compress the O-ring. These are included in the total force with the HOPA force when performing the stress and displacement analysis of the Pawl Arm.

The calculated HOPA force was entered into SolidWorks SimulationXpress as the applied force. The maximum stress and displacement at the point of applied force was generated by SolidWorks as shown in

Figure 11.

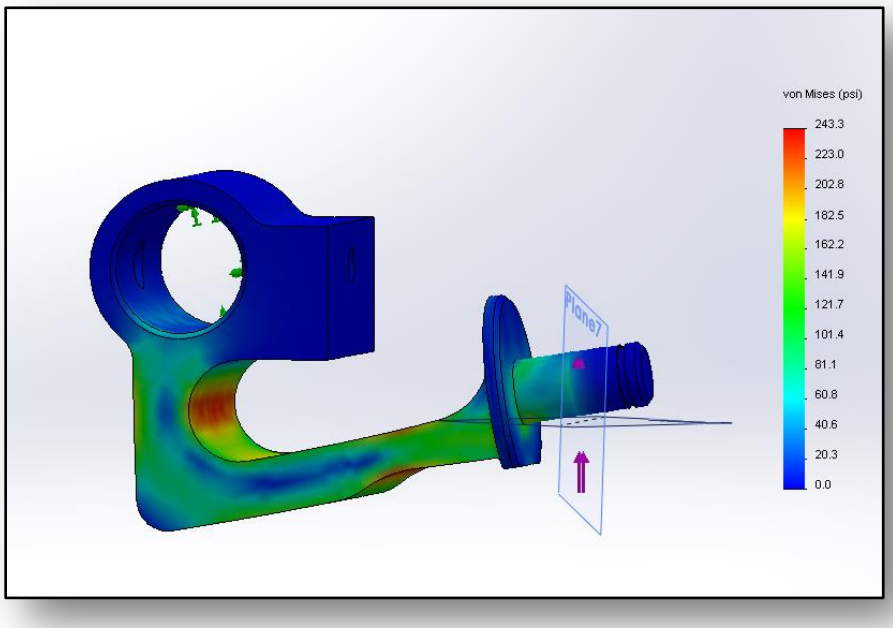

Figure 11: Stress Calculations Completed by SolidWorks SimulationXpress

Chapter 3: O-Ring Test Standards

O-Rings have no specifications as to how they will act under applied compression and temperature scenarios. There is currently no available data as to how multiple types of O-rings, tested under the same standardized system, will deflect due to an applied force, what temperatures will cause failure, the materials an O-ring can expel under temperature and compression, O-ring surface metrology in relation to adhesion, etc. In order to better understand all of these parameters, experiments were performed to gather the aforementioned data to form a basis of direct comparison between different O-ring compounds. The interpretation of this data allows for confident down-selection of candidate O-rings suitable for our application.

3.1 O-Ring and Interface Test Subjects

Sixteen types of O-rings and twelve different interfaces were tested for adhesion, resulting in 550 tests. The properties of the various O-rings and interfaces are shown in Table 1 and Table 2**.** Due to the long procurement process, all O-rings and interfaces were chosen by our LL advisors before the start of the MQP. Most O-rings were tested with and without vacuum baking to identify the hypothesis that vacuum baking reduces adhesion. The vacuum baking process defined was 7 days at 115 C°. Some of the O-ring types were tested in FEP encapsulation. FEP (fluorinated ethylene propylene) is a form of Teflon shrink tubing, which would be placed over the O-ring sample and shrunk to fit the O-ring. S7440_050, CV2289, V0986, were all tested as regular and FEP encapsulated O-rings, and Creavey O-rings were tested strictly as a FEP encapsulated O-ring. Some of the O-rings are also custom fabricated by injecting RTV or

silicones into thick walled Teflon tubing with the appropriate inner diameter. All O-rings are made of polymer based substances, and therefore are very vulnerable to chemical interactions and inconsistencies within themselves. O-Ring composition can vary depending on the temperature the O-ring is stored at, how long it cures for, the humidity and pressure at storage, etc. The O-ring spec sheets can be found in Appendix E. All O-rings were tested against chemical film machined aluminum interfaces to allow for consistent comparison.

Table 1: Table of O-Ring Types and their Identifying Information

O-Ring Name	Manufacturer	Description	Durometer
V0986 (Viton)	Parker	Fluorocarbon based O-ring for high vacuum and high temperature situations	50
SCV2585 (Custom O-ring)	Nusil	Silicone based O-ring for use in applications requiring ultra-low outgassing	40
S0899	Parker	Silicone based O-ring for low temperature applications	50
E1100	Parker	EPDM based rubber O-ring	50
LM151	Parker	Fluorosilicone based O-ring for low temperature applications	50
S0469	Parker	Silicone based O-ring for low temperature applications	40
RTV566 (Custom O-ring)	Momentive Performance	Silicone based O-ring for low outgassing applications	60

	Materials		
S0802	Parker	Silicone based O-ring for low temperature applications	40
CV2289 (Custom O-ring)	NuSil	Silicone based O-ring	40
JABAR 40 Duro	JaBar	Silicone based O-ring	40
S7440_050	Parker	Silicone based O-ring with a hollow inter-diameter of 50 mils	40
C0267	Parker	Neoprene based O-ring for low temperature applications	50
V0986_P14	Parker	Silicone based (Viton) O-ring with Parkerslick P14 coating	50
FEP+SIL_HC_30	Creavey	Silicone based O-ring with a hard Teflon outer shell and hollow inner diameter of 30mils	90
FEP+SIL_HC_50	Creavey	Silicone based O-ring with a hard Teflon outer shell and hollow inner diameter of 50mils	90

The processes and requirements of each type of surface finish can be found in Appendix D. The coatings and finishes were chosen for the likelihood of low adhesion as described by the manufacturer's information. Some surfaces, such as aluminum, were tested with various finish types to find which type of finish resulted in the lowest adhesion. All interfaces were tested

against V0986 O-rings to allow for consistent comparison. The best surface performers were paired with the promising O-ring type.

Table 2: Table of Interface Types and their Identifying Information

Interface Name	Description
CFM (Chemical film, typical machined finish)	An aluminum top plate with a typical machined finish and chemical chromate coating.
CFB (Chemical film, Bead Blasted)	An aluminum top plate with a bead blasted surface finish and chemical chromate coating.
CFP (Chemical film, Polished)	An aluminum top plate with a polished finish and chemical chromate coating.
NH1	An aluminum top plate coated with General Magnaplate's Nedox NH-1 coating for resistance to wear and corrosion.
SANF	An aluminum top plate with Sanford Quantum Hard coat and Sanford Hard lube coating for high abrasion resistance.
DICR	An aluminum top plate with Dicronite coating for a low outgassing and low coefficient of friction surface.
HTR	An aluminum top plate with a Tufram HTR coating by General Magnaplate for a low adhesion coating.

TAPE	An aluminum top plate with Silver Teflon Tape applied for a low adhesion, low solar absorption surface.
INVAR	An invar top plate with a typical machined surface finish.
INVAR BLASTED	An invar top plate with a bead blasted surface finish.
SF-2	An invar top plate coated with General Magnaplate's Nedox SF-2 coating for hardness with lubricity.
N615W	An invar top plate coated with General Magnaplate's Nedox N615W coating for a low adhering coating.

3.2 O-Ring Sample Preparation

Each O-ring test sample required proper preparation before testing. Prior to physically assembling the O-ring sample any treatments or coatings, such as vacuum baking, were applied to the samples. The test sample set-up was comprised of several components including the O-ring, top plate, bottom plate, four socket head cap screws, and four 0.014" thick washers, as shown in Figure 12. The socket head cap screws held the top and bottom plates against the washers to establish constant 0.013" displacement of the O-ring. The O-ring rested in the dovetail groves of the bottom plate, and touched the top plate. For DMA testing, thermal survival

testing, and thermal adhesion testing, the following procedure was performed. The samples were assembled in a clean room environment to greatly reduce particulate contamination.

Figure 12: O-Ring Testing Set-Up

All materials brought into the clean room were cleaned with isopropyl alcohol or vacuumed for particulates before entering. The washers and screws were subjected to a vapor degrease and isopropyl ultrasonic bath for 5 minutes. The O-rings were cut into approximately 1.5" long pieces and then wiped with isopropyl alcohol. After cleaning the O-rings, they were left to sit for a minimum of 15 minutes, to allow any remaining isopropyl alcohol to evaporate. The O-rings were then positioned into the dovetail groves in the bottom plate. The washers were placed on the bottom plate around the screw holes, and the top plate placed on top of the O-rings as shown in Figure 13.

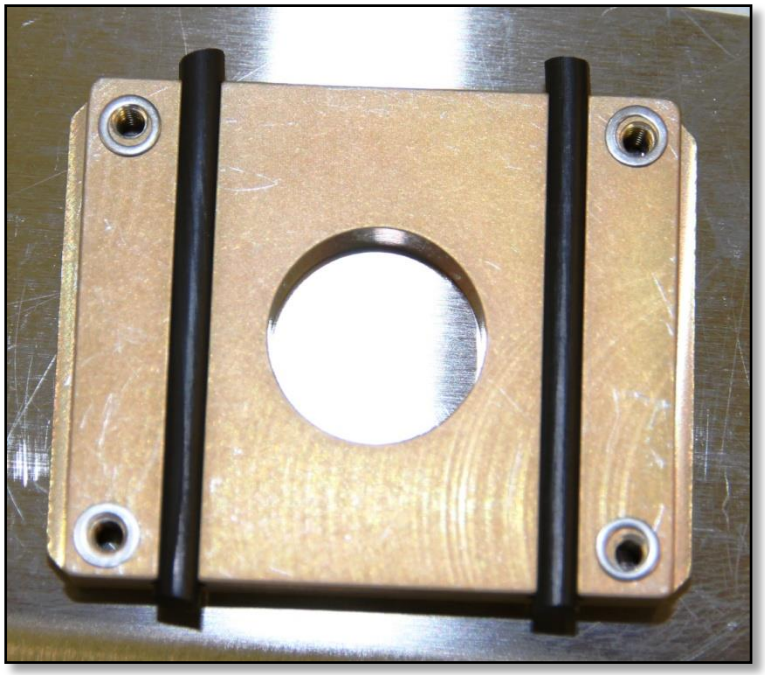

Figure 13: O-Ring Bottom Plate with O-Rings and Washers

The screws were installed through the top plate and into threaded into the bottom plate and were torqued to 2 ft-lb in a 'X' pattern to ensure that each sample had the same applied compression force on the O-ring. A small alignment test fixture was used to center the top plate over the O-rings while placing the top plate upon the O-rings. The O-ring test set-ups were then sealed in bags and left in contact for 7 days at room temperature before testing.

After the samples were tested, the top plates were cleaned with tetrahydrofuran (THF) in a solvent hood using clean room swabs. This was done to remove any O-ring residue deposited on the top plates. The top plate samples were also cleaned in an ultrasonic isopropyl bath between 5 and 10 minutes, then dried with a nitrogen gun and left to air dry to evaporate any remaining liquid. The O-rings were also re-cleaned by being wiped in isopropyl alcohol and left to dry for 15 minutes. O-Rings were only retested on the same interface it had been previously tested on to

avoid cross contamination. The samples were then fully reassembled in the clean room to be retested.

3.3 Dynamic Mechanical Analyzer Testing for Adhesion

A Dynamic Mechanical Analyzer (DMA) was used to test the O-ring samples for adhesion using a custom fixture, as shown in Figure 14. The DMA load shaft had a hemispherical interface that would pilot on the hole within the top plate of the adhesion specimen. The load shaft would then be secured to the top plate by hand tightening the nut. The O-ring sample was aligned to the DMA load shaft to ensure the load shaft was perpendicular to the top plate of the sample. This was verified by lifting upon the DMA load shaft to ensure the bottom of the adhesion specimen baseplate lifted in a parallel motion from the DMA platen. After this check, the adhesion test sample's bottom plate was clamped to the DMA platen by screwing down the two side clamps. The sample was held in place by one test operator, while the other screwed down the screws to ensure the adhesion specimen didn't move. The four socket head cap plate screws were carefully removed in a cross-hatch pattern, while the top plate was compressed manually to ensure no movement of the plate during screw removal. The DMA was prompted to start applying force and collecting data via the test computer. The DMA load shaft, top plate, bottom plate and O-rings can be seen in Figure 14 below, in which the top plate has just lifted off the O-rings during the test.

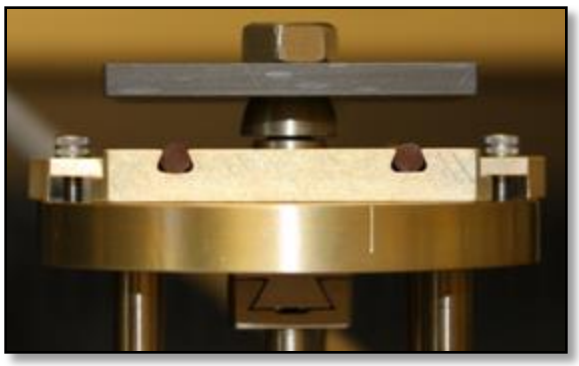

Figure 14: DMA Test as the Top Plate is Lifting

The DMA was checked for accuracy at the start of each day's testing to ensure consistency between the tests by measuring the force of a top plate without any adhesion (i.e., no O-ring). For testing O-ring adhesion, the DMA was programmed to apply ramp to 0.1 N of force at a rate of 0.25 N/min in the negative y-direction of the DMA (upward lift of the top plate away from the O-ring). After reaching 0.1 N (which is about half the nominal weight of an aluminum top plate), the DMA would then ramp to 18 N of force at a rate of 5 N/minute (upwards). In all tests, the top plate separated prior to reaching 18 N. Using TA Universal Analysis, the DMA reported the applied force on the test sample, and stopped applying force when the sample yielded, as shown in Figure 15**.**

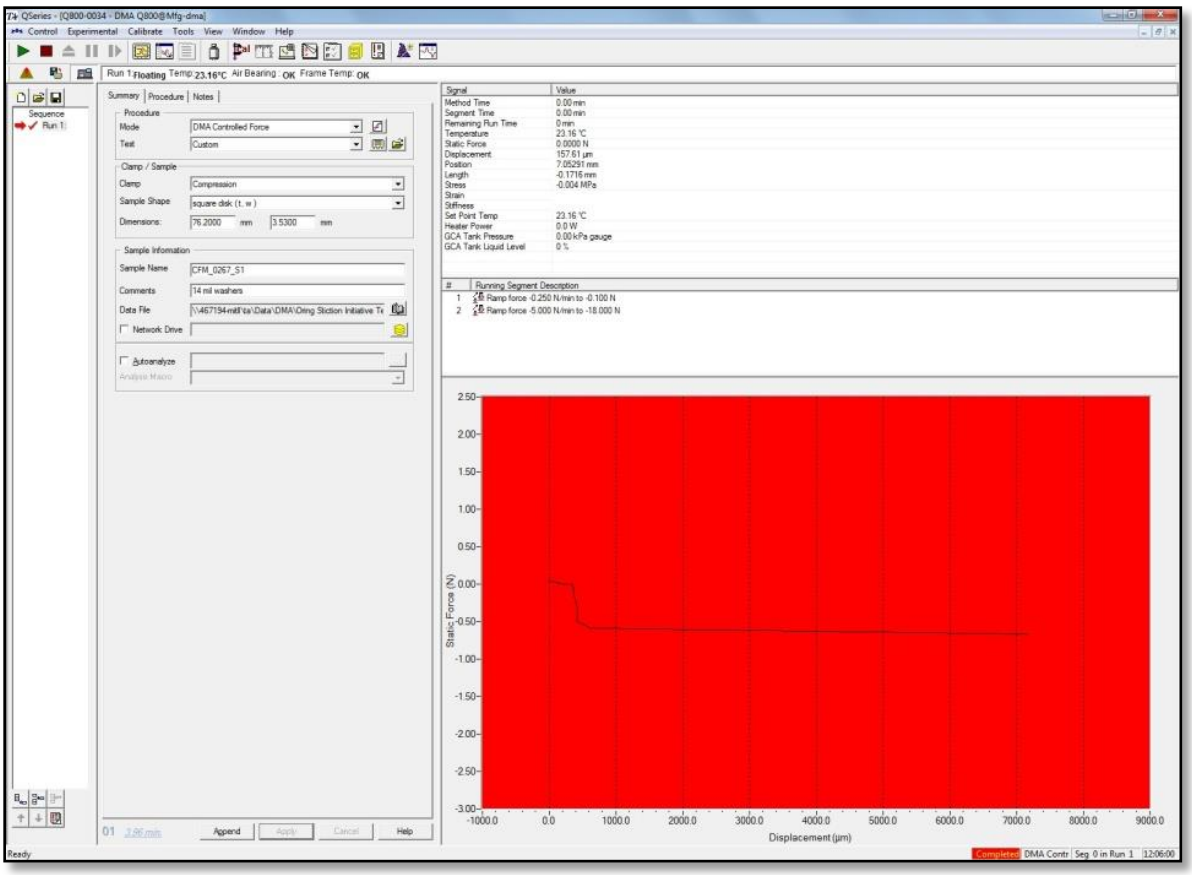

Figure 15: TA Analysis Software for Performing DMA Tests

The full procedure and computer set-up was established by our LL advisors and WPI summer student Brian Walker and is described in Appendix A. The program outputs a data file to a TA Universal Analysis program, in which the adhesion force of the O-ring can be extracted as shown in Figure 16**.**

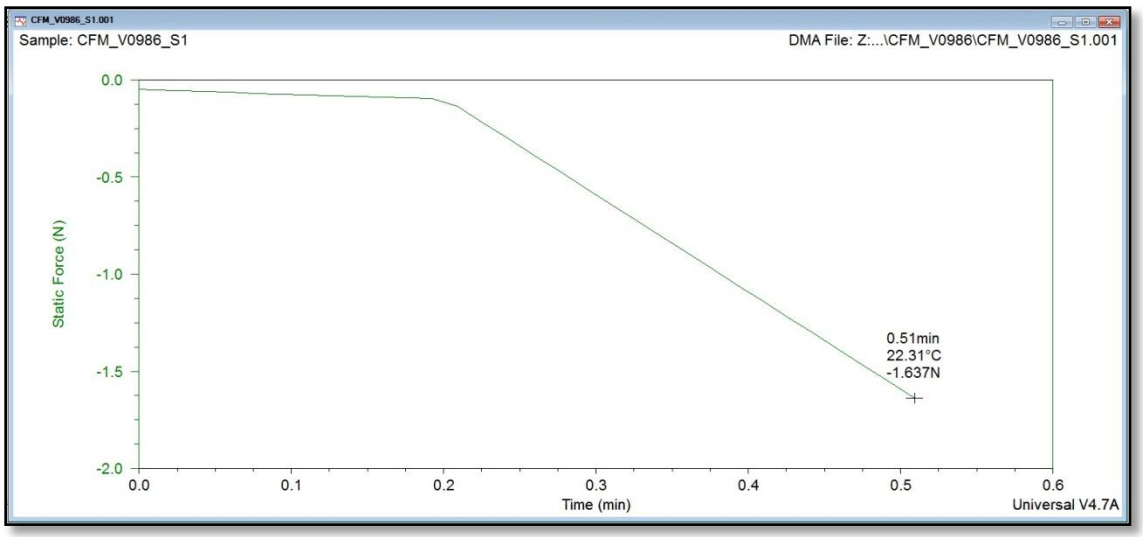

Figure 16: Adhesion Data Retrieval in Universal Analysis

Each test was video recorded with a high speed video camera and examined for "uneven pops" or cases where the top plate lifted off of the O-rings unevenly. Uneven pops were excluded from the data, as the applied force recorded to lift the plate is no longer in strictly tensile, but rather includes a peel force. All of the results were entered into a Microsoft Excel spreadsheet, part of which is shown below in Figure 17.

. Besides measured adhesion force, there was a variety of other data recorded such as: the date the samples were prepared, the date tested, the universal analysis filename, the total days of O-ring compression, the scaled normalized adhesion force in lbf/inch, the standard deviation. The comments section included whether the top plate lifted evenly, what time it was tested at, whether all washers were present after the test was completed, whether residue was found on the top plate from the O-ring, along with any other important notes.

Stiction vs O-ring								
Prepared	Tested	Filename	O-Ring Compression (mils)	Duration of Compression (days)	Adhesion Force (N)	n Force - Calibration 0 (N)	Adhesion Force Used in Plots (lbf/in)	Standard Dev/Comments
8/7 & 8/29		CFM_V0986_Sx	14 mils		2.1117	2.0622	0.1563	0.0289
8/7/2012 at 2:30pm	8/15/2012	CFM_V0986_S1		8	1.4670	1.4175	0.1099	even lift, tested at 1:53pm, all washers present, no visible residue
8/7/2012 at 2:30pm	8/15/2012	CFM_V0986_S2		8	2.1428	2.0933	0.1606	even lift, tested at 1:57pm, all washers present, no visible residue
8/7/2012 at 2:30pm	8/15/2012	CFM_V0986_S3		8	2.1444	2.0949	0.1607	even lift, tested at 2:04pm, all washers present, no visible residue
8/7/2012 at 2:30pm	8/15/2012	CFM_V0986_S4		8	1.8009	1.7514	0.1350	even lift, tested at 2:08pm, all washers present, no visible residue
8/7/2012 at 2:30pm	8/15/2012	CFM_V0986_S5		8	3.1430	3.0935		uneven lift, tested at 2:13pm, all washers present, no visible residue
8/29/2012 at 11:45am	9/6/2012	CFM_V0986_S6		8	1.8790	1.8295	0.1408	no residue, even lift, 1 washer stuck, twisted top plate, all washers present
8/29/2012 at 11:45am	9/6/2012	CFM_V0986_S7		8	2.6440	2.5945	0.1981	10 mil shim under clamps, no residue, no twis top platet, O-ring twisted, even lift, all washers present
8/29/2012 at 11:45am	9/6/2012	CFM_V0986_S8		8	~~1.2880~~	1.2385		high twist in plate, no residue, uneven lift, twisted O-ring on side that lifted first, all washers present, recommend not using this data point
8/29/2012 at 11:45am	9/6/2012	CFM_V0986_S9		8	2.0586	2.0091	0.1543	slight twist in plate, even lift, no residue, left O-ring twisted, all washers present
8/29/2012 at 11:45am	9/6/2012	CFM_V0986_S10		8	2.5490	2.4995	0.1910	even lift, slight twist in plate, no residue, O-rings good, all washers present

Figure 17: O-Ring Adhesion Measurement Spreadsheet Example

The adhesion force was calculated by the force reported by TA Universal Analysis, minus the weight of the top plate. The adhesion force calibration column was calculated by subtracting the amount of force measured by TA Universal Analysis to lift the top plate with no O-rings in the base plate, minus the weight of the top plate. The columns that are highlighted above are tests which either resulted in an uneven lift or some form of malfunction with the sample, i.e. twisted O-rings or a twisted top plate. The full spreadsheet can be found in Appendix G**.**

3.4 Dynamic Mechanical Analyzer Testing at Hot and Cold Temperatures

The DMA was also utilized to test O-rings at hot and cold temperatures for adhesion of the O-rings considered to be our best O-ring candidates. The hot testing was conducted at +50 °C, and the cold at -50 °C. These temperatures were used to determine the worst case adhesion under realistic thermal conditions for the Launch Latch. The procedure completed for hot and cold testing was the same as room temperature DMA testing, except the DMA's furnace feature was activated to create a thermal chamber to test the samples under. Due to the furnace enclosing the samples, no videos were taken for thermal tested samples. For both hot and cold testing, the samples were applied to a thermal soak at the given temperature for an hour, then prompted to

separate the top plate from the O-rings, measuring how much force it took to cause the separation. The test plan can be found in Appendix A. It was hypothesized that cold testing would result in higher adhesion values, particularly for O-rings with large amounts of residue, as this has been an observed trend in past O-ring adhesion scenarios.

3.5 Thermal Survival Testing

Thermal survival tests were conducted on the O-ring samples to evaluate performance under extreme cold situations. An O-ring type was placed into one of the dovetail grooves of the test sample, similar to DMA testing, and another O-ring type placed into the adjacent groove. Washers are then placed on the bottom plate, and the top plate placed on top of the washers. Four screws were then used to compress the top plate onto the O-rings. The screws were applied with 2.6 in-lbf of torque via a torque wrench. The samples were then placed in a thermal chamber which soaked the samples to -70 °C for 120 hours. The samples post thermal soak were examined at 50X magnification using a Keyence microscope, and photographed to record the effects of thermal testing on the O-rings. For O-rings with questionable deformation, three-dimensional photos were also taken with the Keyence for further examination. The Launch Latch is required to open under a temperature warmer than -50 °C which makes this test very conservative. It was hypothesized, based on the O-ring data sheets that V0986, C0267, E1100, S0802, S0469, and JaBar40 would fail thermal survival testing. Each of those O-ring types was reported in their data sheets to fail at temperatures above -50 °C.

3.6 Stiffness Testing

The stiffness testing was completed by Peter Anderson, a laboratory technician at LL. The technician placed the sample in the Instron force measurement device and aligned the top piston of the Instron with the top plate of the O-ring test sample. The technician then ensured that the O-ring was in the dovetail groves of the bottom plate by applying a light amount of pressure to the top plate. Once the O-rings were set, the Instron was backed off from the top plate. The machine was then zeroed by manipulating the Instron such that the force on the top plate read by the machine was 0.005 lbf. The Instron was then programmed to compress the top plate onto the O-rings at a given rate of approximately 5 mils per minute, until the sample reached 30 mils of deflection or the sample yields. The data collected by the machine was plotted as force (lbf) versus the deflection (inches). Two or three tests were run per sample depending on the linearization of the O-ring stiffness. It was expected that O-rings with higher stiffness would also have higher durometer.

3.7 Durometer Testing

The Shore A durometer of each O-ring type was tested using an Intron E1000. The Instron measured durometer using a pin-point measure of resistance within the O-ring. Three durometer measurements were taken for each O-ring type and averaged. The durometer measurements were then compared to adhesion, and stiffness data to explore any correlations between O-rings and their durometer. Both the regular and the vacuum baked samples of O-rings were tested. It was hypothesized that there would be little to no variation in durometer between the regular and vacuum baked samples of the O-rings.

3.8 Outgassing Testing

Outgassing testing was performed on the O-rings by various outsourced testing sites. The complete testing procedure used by Outgassing Services International to test the O-rings can be found in Appendix B. The test procedures were conducted by the American Society for Testing and Materials (ASTM) International standards for outgassing, E595-07. E595-07 is used to describe the allowable parameters for total mass loss (TML) and collected volatile condensable materials (CVCM) of a given material in space conditions near optics. As stated by the ASTM International test designation, TML "is the total mass of a material outgassed from a specimen at a specified constant temperature and operating pressure for a specified time. TML is calculated from the mass of the specimen as measured before and after the test and is expressed as a percentage of the initial specimen mass ("Standard Test Method", 2007)". The other parameter measured, CVCM, is defined as "the quantity of outgassed matter from a test specimen that condenses on a collector maintained at a specific constant temperature for a specified time. CVCM is expressed as a percentage of the initial specimen mass and is calculated from the condensate mass determined from the difference in mass of the collector plate before and after the test ("Standard Test Method," 2007)". The test method required by E595 standards can be found in Appendix B. The test requires at TML and CVCM report values less than or equal to 1.00% and 0.10% respectively in order to pass as a low outgassing material. Our recommended O-ring selection is required to meet the same standard.

3.9 Optical Metrology and Surface Roughness

The interfaces were measured for surface roughness by using a Zygo NewView interferometer. Average surface roughness, route mean squared roughness, skewness, kurtosis, and average

maximum height of the profile were extracted. Visual surface texture, average roughness and adhesion values were compared and conclusions were made. It was hypothesized that the lower the average surface roughness, the higher the adhesion. It was theorized that the O-ring residue under compression cannot flow into the smaller areas of a rough surface, and therefore would make contact with less of the surface than that of a less rough surface. It was also conceived that the pores in a rough surface may be able to capture O-ring residue released by the O-ring while under compression, and may make the effect of O-ring residue less pertinent on adhesion.

3.10 Residue/Squish Testing

O-Ring residue was examined as a possible warning sign for an increased source of adhesion. Half-inch sections of O-ring samples were squish tested against a silicone plate, compressed to that plate at a force of 40 lbf for twenty-four hours. Ellipsometry measurements of the residue were taken to measure the residue thickness. The squish test residue samples were then air-baked at 200 °C for 72 hours to see if this lessened or eliminated the residue thickness. Ellipsometry measurements were performed again on the samples post-baking to measure the amount of remaining residue. The samples were then baked at high vacuum at 200 °C for a week to remove any further residue. It was hypothesized that baking or vacuum baking the O-rings may lessen the amount of material that flows out of them which may reduce O-ring adhesion. If his were true then the residue thickness collected on the silicon plates would decrease.

Chapter 4: O-Ring and Interface Data Analysis and Results

This chapter presents the data collected by the various tests that were conducted, and their implications on O-ring adhesion. The analysis of adhesion in reference to all O-rings and interfaces is examined, as well as outgassing, stiffness, O-ring residue, and thermal survival testing. The analysis of the tests resulted in the narrowing of O-ring and interface combination in order make a final recommendation for use with the ST.

4.1 Adhesion Analysis

Adhesion data was collected for all O-ring samples on a common interface, chemical filmed aluminum. Each O-ring type was tested in both its regular and (if available) vacuum baked condition as shown in Figure 18. The O-rings were compared to determine which ones had the least amount of adhesion. The vacuum baked O-rings results were the most applicable as space payloads by LL standards, must use vacuum baked parts. In most cases, vacuum baking decreased O-ring adhesion. However in some cases O-rings increased in adhesion, specifically for E1100, LM151, V0986, and C0267. Notably, none of the O-rings that increased in adhesion force were silicone based O-rings. For each set of data shown, error bars were applied with a 95% confidence level that the O-ring's adhesion force would occur below that. The highest value given by the 95% confidence interval was chosen to plan for the worst case scenario of O-ring adhesion. The O-rings with the least amount of adhesion were all three FEP encapsulated O-rings, along with RTV566, SCV2585, S0469, and CV2289.

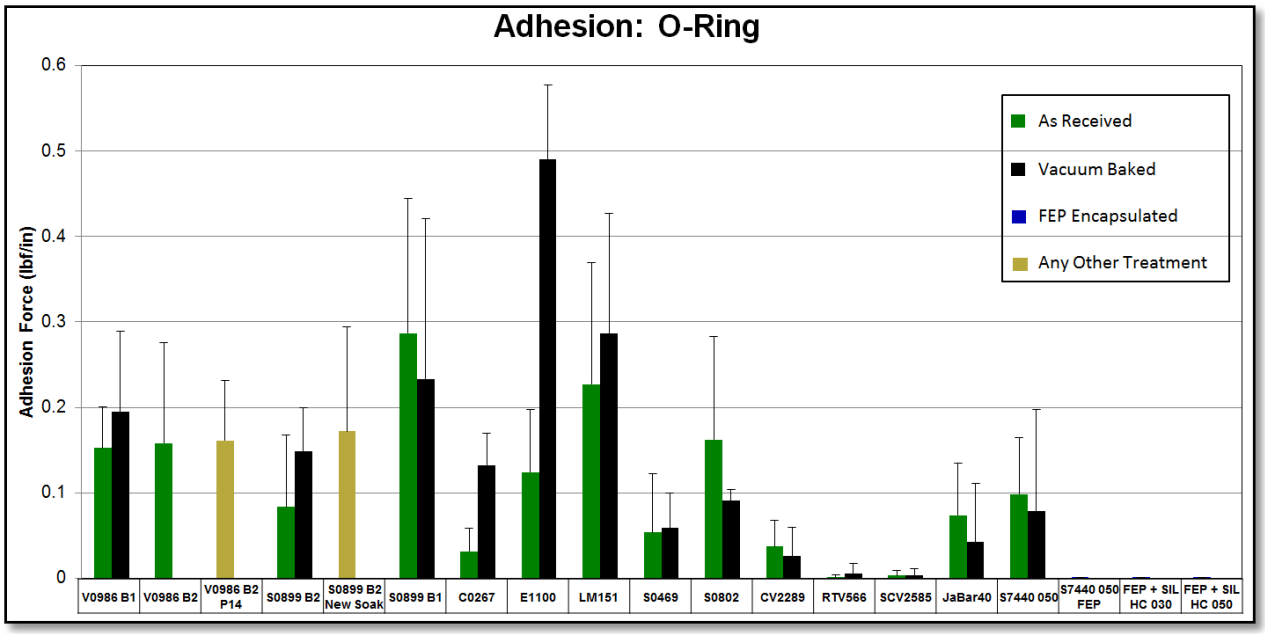

Figure 18: Adhesion of All O-Ring Types on Chemical Film Aluminum

Adhesion values were also compared to the various interfaces against a common O-ring, V0986-50, as shown in Figure 19. These tests were used to compare the various interfaces against one another for low adhesion. The two different base plate materials aluminum-6061 and invar-36 are shown in blue and red respectively. The two surfaces with the lowest adhesion values were HTR on chemical film aluminum, bead blasted chemical film aluminum, and Nedox 615 White on invar.

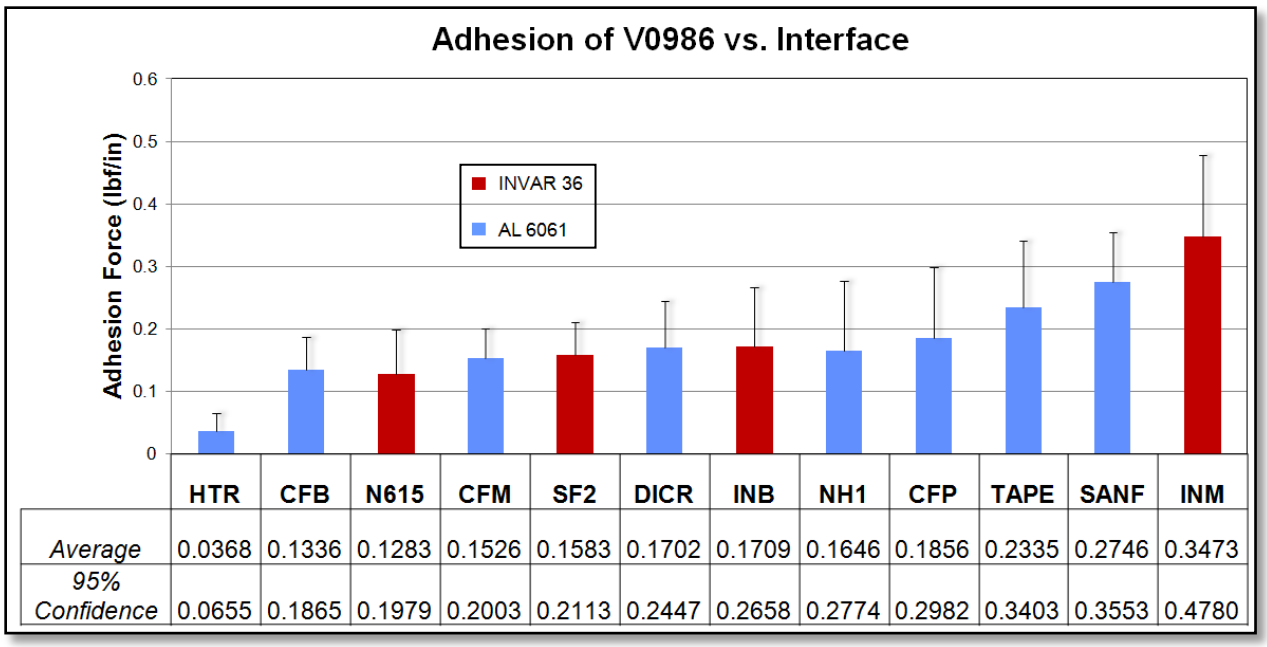

	HTR	CFB	N615	CFM	SF2	DICR	INB	NH1	CFP	TAPE	SANF	INM
Average	0.0368	0.1336	0.1283	0.1526	0.1583	0.1702	0.1709	0.1646	0.1856	0.2335	0.2746	0.3473
95% Confidence	0.0655	0.1865	0.1979	0.2003	0.2113	0.2447	0.2658	0.2774	0.2982	0.3403	0.3553	0.4780

Figure 19: Adhesion of V0986 on All Interface Types

It is important to note that adhesion could vary between batches of O-rings, shown in Figure 20. An O-ring batch is a group of O-rings made at the same time from the same compounds and mixture. When a secondary batch of O-rings is made, it can experience different forming of the polymers within the O-ring, or worse contain different mixture percentages of compounds in the mixing process. In the case of S0899, the average adhesion (lbf/inch) of batch two was less than a third of the average adhesion of batch one, non-vacuum baked. The batches also did not react similarly to vacuum baking in terms of average adhesion, batch 1 decreased and batch 2 increased. S0899 was also tested to measure the effect of isopropyl alcohol on O-ring adhesion. Samples of S0899 were soaked in isopropyl alcohol for 24 hours and hung to dry for a minimum of 2 days. The S0899 soaked samples had an average adhesion of more than twice the non-soaked samples. The average value for S0899 soaked was based off of samples with even lift, however if the isopropyl alcohol created inconsistencies in the continuity of adhesion on the

O-ring surface, causing the uneven lift, the average adhesion value for all data collected would be 0.2101 lbs/inch, almost three times the original average adhesion.

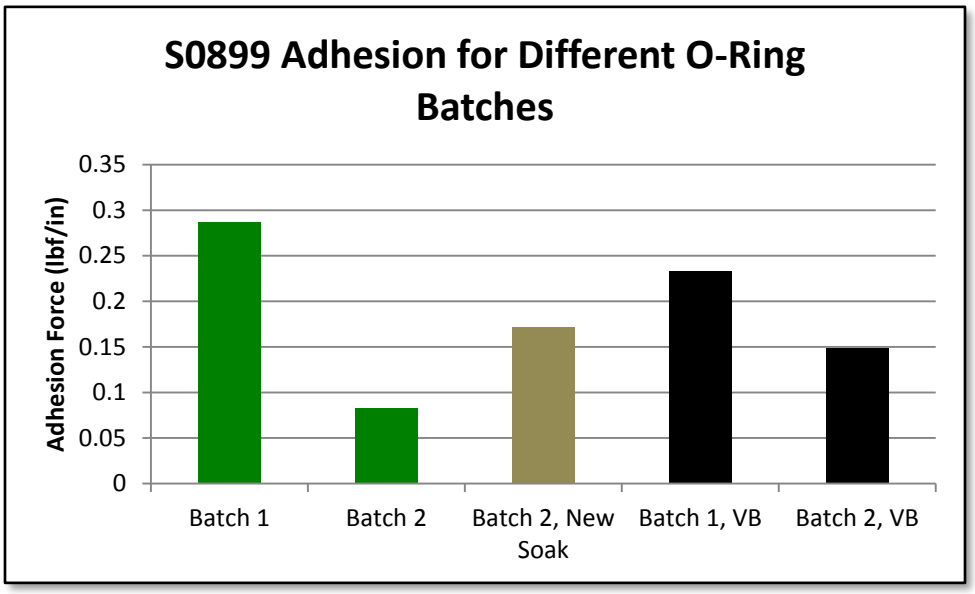

Figure 20: S0899 Adhesion for Different O-Ring Batches.

The adhesion results were compared with other forms of data, including O-ring residue and surface roughness, and can be found in those respective sections.

4.2 Thermal Survival Testing Analysis

Images were taken at 50x magnification of the O-ring surfaces before and after thermal survival testing. For all O-rings examined (except Parkerslick and Creavey), E1100 and JaBar40 were the only O-ring types which after being thermal tested, resulted in severe cracking, pitting, and therefore failure of the O-ring. E1100 exhibited cracking and lines on the O-ring post testing as demonstrated in Figure 21. The result caused us to rule out E1100 O-rings as a possible recommendation for use in the Launch Latch. E1100 was the only EPDM based O-ring tested,

which may have contributed to the thermal survival results. JaBar40 also performed poorly exhibiting pits in the material.

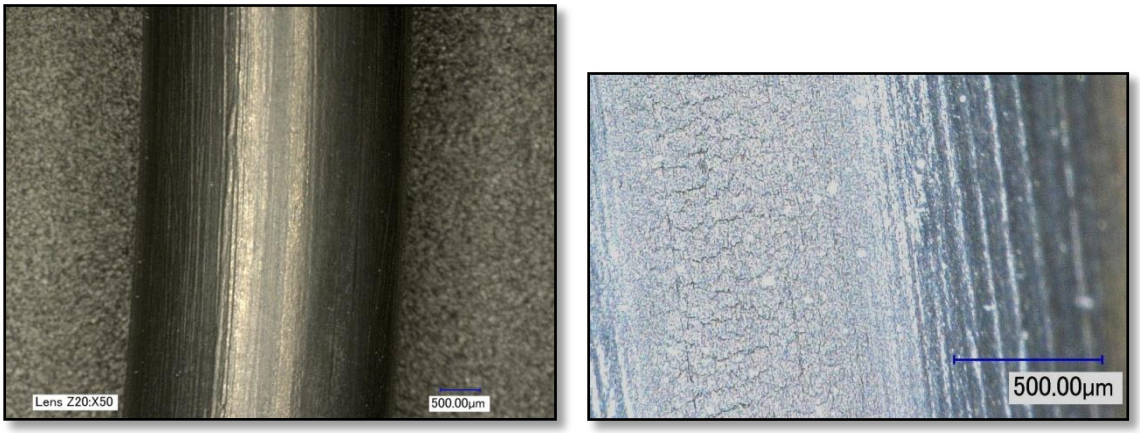

Figure 21: Thermal Survival Before and After Pictures of E1100

Some O-rings exhibited change in their form due to thermal testing, but none as drastic as E1100 or JaBar40. V0986 O-rings when analyzed by the Keyence microscope as a 3D shape produced images that showed the O-ring as flattened post thermal testing shown in Figure 22. O-Ring flattening was not seen as a failure point, but more so as a normal deformation of the O-ring due to temperature and compression, the O-ring would still be expected to perform correctly. Though the hypothesis stated that many more types of O-rings would fail, only E1100 and JaBar40 exhibited signs of severe failure. It is possible that the thermal testing which O-rings undergo for their specification sheets and whatever safety margins are included are more rigorous than our testing scenario. However, the thermal survival test we conducted was designed to specifically address a realistic environment that these O-rings may be subjected to and is therefore a more relevant result for our purposes.

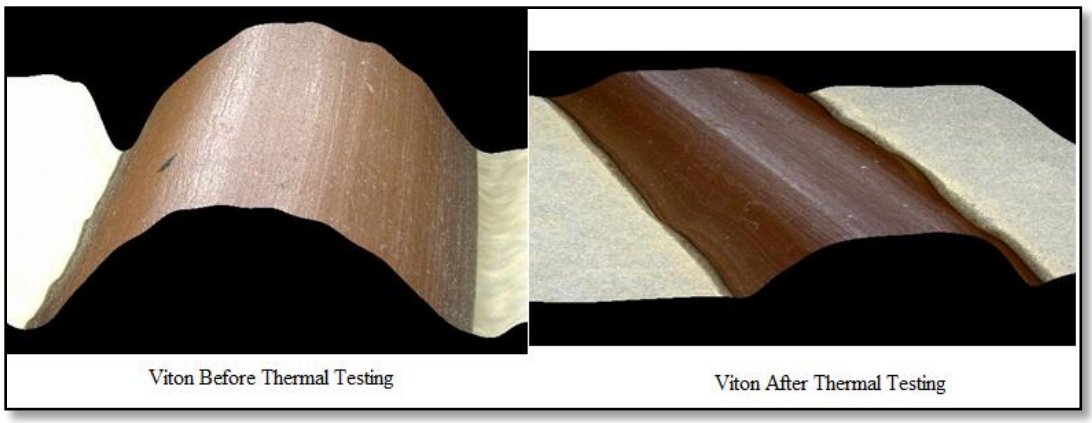

Figure 22: 3D Image of V0986 Before and After Thermal Testing

4.3 Stiffness and Durometer Analysis

Stiffness data was collected for each type of O-ring. The data collected by the Instron was analyzed for the force required to deflect the sample between 0.005 inches and 0.020 inches. A best fit line was fitted for both polynomial and linear equations and an R^2 value calculated to determine the likeness of the equation, as shown in Figure 23. Almost all O-rings were fit well by a linear equation, which was demonstrated by an R^2 value of 0.99 or greater. The O-rings that did not react linearly to applied force tended to the lower durometer O-rings. All of the force vs. deflection data, including equations, calculated stiffness, durometer, and correlation graphs can be found in Appendix G**.**

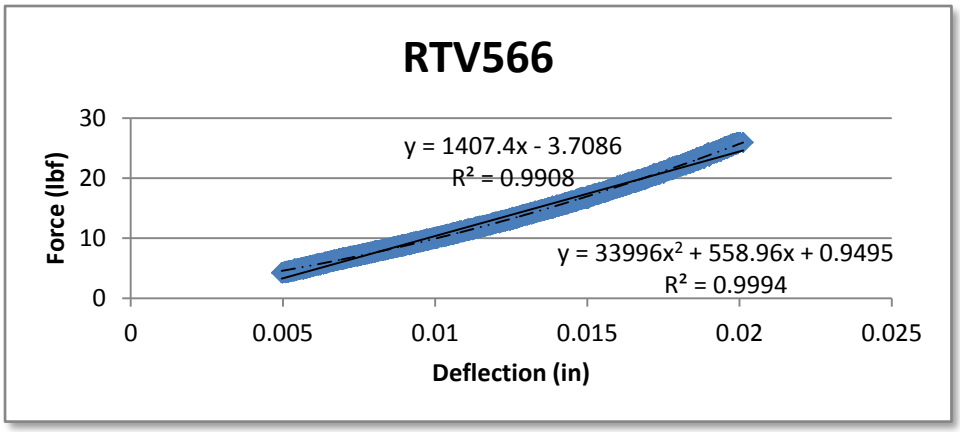

Figure 23: Force vs. Deflection Data for RTV566

Each O-ring was recorded at 0.010 inches to compare the required force per unit of deflection. Ten mils was chosen as an analysis point as that is the defection of the O-ring when compressed in the Launch Latch. The numerical results were used to determine which O-rings require greater force to compress the same distance. The lowest force per deflection required was achieved by S7440 with varying inner diameters, SCV2585, CV2289, and S0469 as shown in Figure 24. The O-rings with the highest stiffness were E1100, RTV566, and all of the FEP encapsulated O-rings. In order to minimize the required force for the HOPA's to hold the Launch Latch closed, we are optimizing low stiffness. O-Ring stiffness was compared to its measured durometer to observe any correlations in the data, shown in Figure 25. The FEP encapsulated O-rings were not included in this measurement, as the FEP encapsulation affects the stiffness of the O-ring regardless of its core O-ring. There is a slight increasing linear correlation between stiffness and durometer which is to be expected.

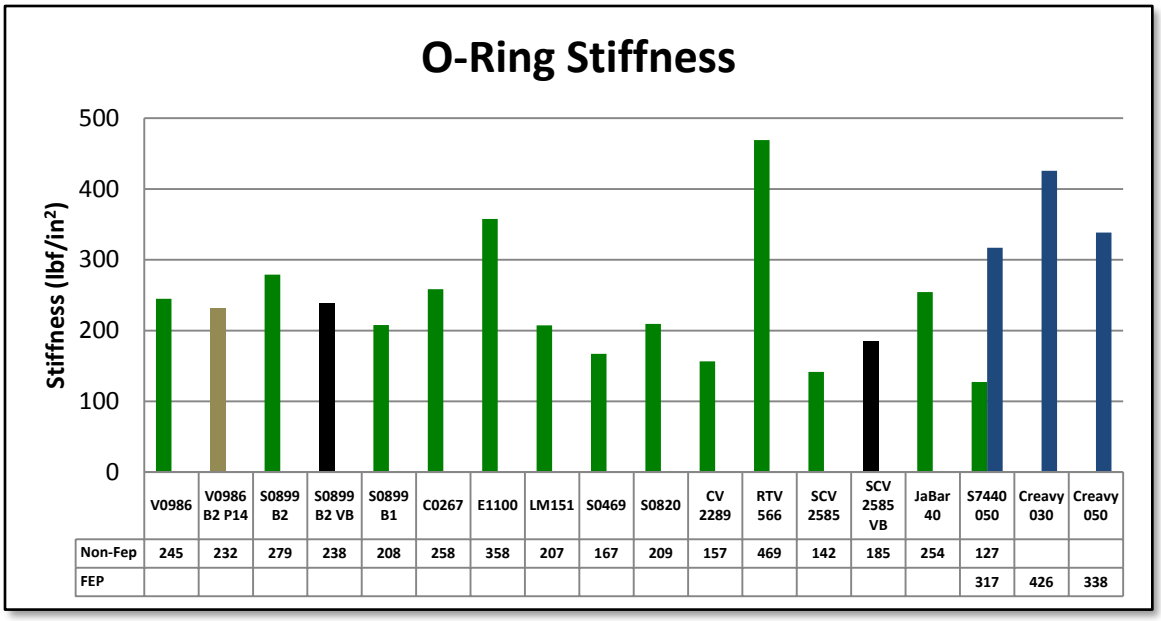

Figure 24: Force Required to Compress O-Rings

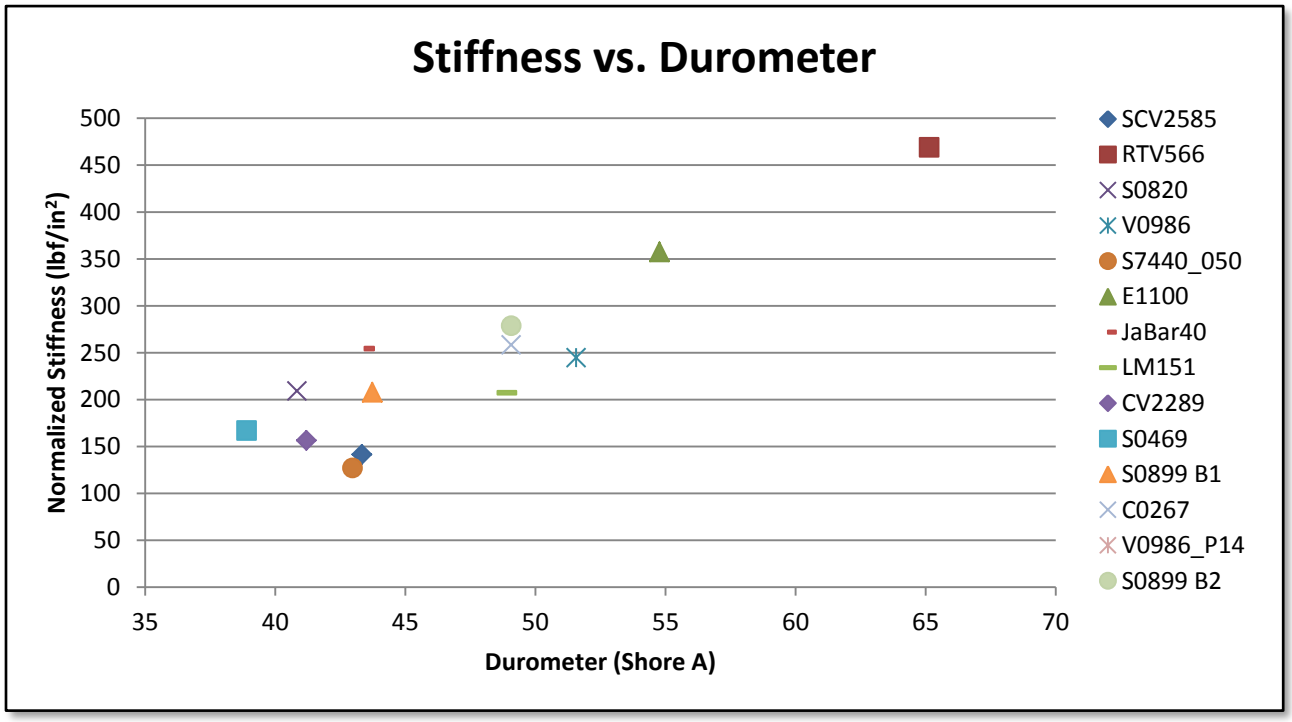

Figure 25: O-Ring Stiffness vs. Durometer

4.4 Outgassing Results

The outgassing results are shown below in Table 3. All O-rings shown below were tested without vacuum baking. The O-rings highlighted are those which passed the ASTM E595-07 standards. The results for V0986, S0899, S0802, CV2289, and SCV2585 were all within the standards of less than 1.00% TML and less than 0.10% CVCM. All other O-rings with the exception of S0469, shown in green, were ruled out as possible candidates for use in the Launch Latch. S0469 resulted in relatively low outgassing values, such that it was theorized that after vacuum baking, outgassing may be low enough to pass E595-07 standards. Vacuum baking has shown to "bake out" low molecular weight materials from the O-rings, resulting in an initial loss of mass that would normally be released during an outgassing test. All O-rings used in space payloads must be vacuum baked pre-flight, therefore a vacuum baked S0469 could be used if chosen. Due to S0469's low stiffness and adhesion, we chose to use it in thermal testing.

Table 3: O-Ring Outgassing Results

O-Ring Material Number	O-Ring Type	%TML, Outgassing Test per E595-07 as received	%CVCM, Outgassing Test per E595-07 as received
V0986-50	**FLUOROCARBON (FKM, FPM)**	**0.22**	**0.02**
S0899-50	**SILICONE RUBBER (VMQ, PVMQ)**	**0.10**	**0.02**
C0267-50	POLYCHLOROPRENE RUBBER (CR), "Neoprene"	8.33	3.35
E1100-50	ETHYLENE PROPYLENE RUBBER (EPM, EPR, EPDM)	8.82	4.34
LM151-50	FLUOROSILICONE (FVMQ)	1.7	0.4
S0469-40	**SILICONE RUBBER (VMQ, PVMQ)**	**1.66**	**0.44**
S0802-40	**SILICONE RUBBER (VMQ, PVMQ)**	**0.06**	**0.01**
CV2289-1	**RTV**	**0.44**	**0.04**
RTV566	**RTV**	**0.1**	**0.01**
SCV2585	**RTV**	**0.08**	**0.007**

Ja-Bar 40 Durometer	**SILICONE RUBBER (VMQ, PVMQ)**	**0.6***	**0.044***
S7440-50	SILICONE 0.050'' ID	0.31	0.11
S7440-50	SILICONE 0.050" ID, FEP Encapsulated	N/A	N/A

* Data from the ASTM 1559 test.

4.5 Optical Metrology and Surface Roughness Results

The data collected by the Zygo microscope was reviewed quantitatively and qualitatively. The surface finishes for aluminum and invar base plates were compared based on their surface roughness and optical metrology. The surface roughness and optical metrology for CFM can be found below in Figure 26. The two surfaces with the least amount of surface roughness were chemical film polished aluminum and silver Teflon tape. The surface with the greatest surface roughness was exhibited by chemical film bead blasted aluminum.

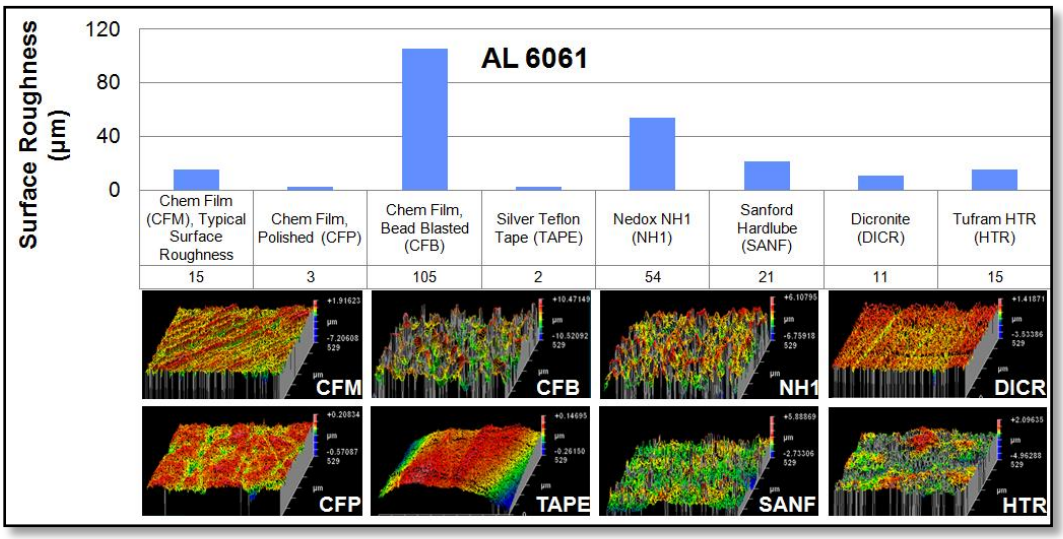

Figure 26: Surface Roughness and Optical Metrology for Aluminum Based Interfaces

The invar surfaces were also compared for surface roughness. The lowest surface roughness was exhibited by invar with no applied surface treatments, and the highest surface roughness was exhibited by the surface coating Nedox SF-2, shown in Figure 27.

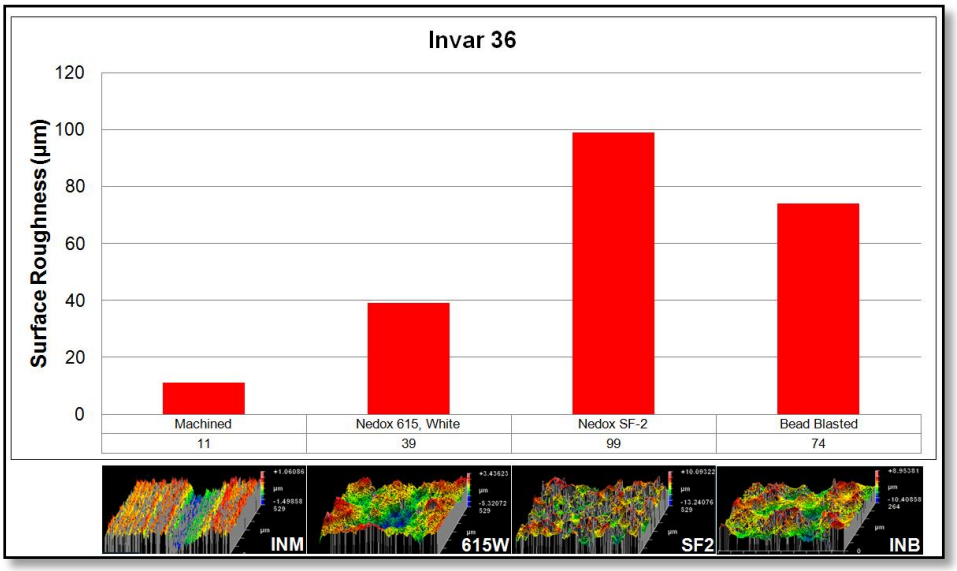

Figure 27: Surface Roughness and Optical Metrology of Invar Based Surfaces

The correlations between surface roughness and adhesion were explored, as shown in Figure 28. No correlation was found between surface roughness and adhesion when adhesion testing was performed on these surfaces with the common Viton O-ring (V0986-50). The two surface types, invar and chemical film aluminum were explored separately (shown in red and blue respectively), as well as O-ring base type (i.e. silicone, neoprene, etc.), and no correlation was found. An example of the lack of correlation is best described by the points around 0.2 lbf/inch on Figure 28. Two of each type of surface all had an adhesion force of about 0.2 lbf/inch, but their surface roughness varied between 20 µm and 110 µm.

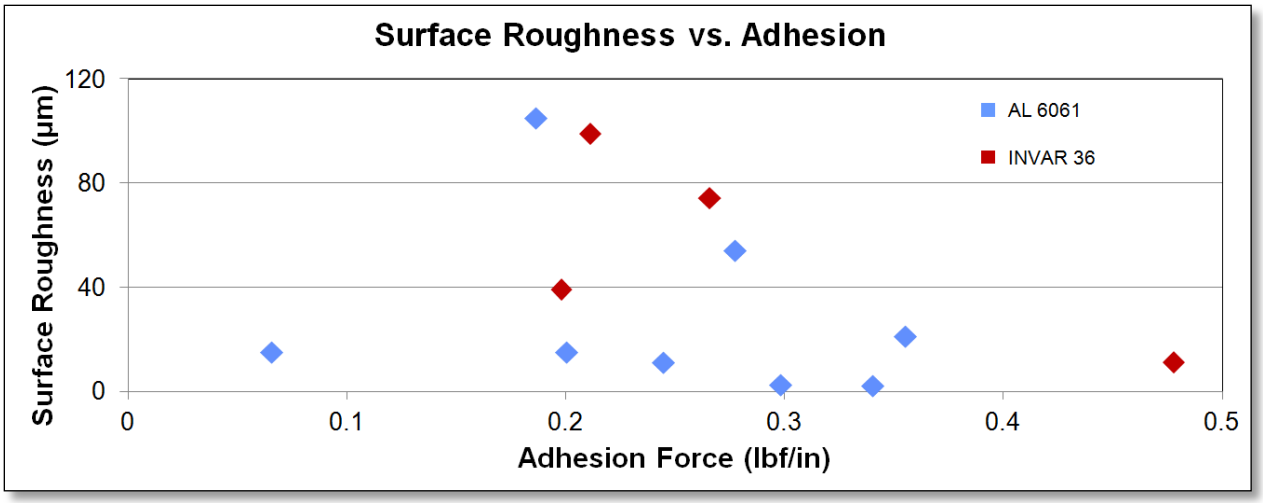

Figure 28: Surface Roughness vs. Adhesion

It is important to note that some surfaces behaved differently with different types of O-rings. We tested SCV2585, RTV566, S0802, S0469 and V0986 on HTR, as HTR was determined to have the lowest adhesion against V0986 versus the other interfaces. The O-rings tested against HTR were determined to have some of the lowest adhesion against CFM. It was theorized that they would perform promisingly against HTR. Although V0986 performed significantly better with HTR than with CFM, S0802 was the only other O-ring whose performance improved on HTR, as shown in Figure 29.

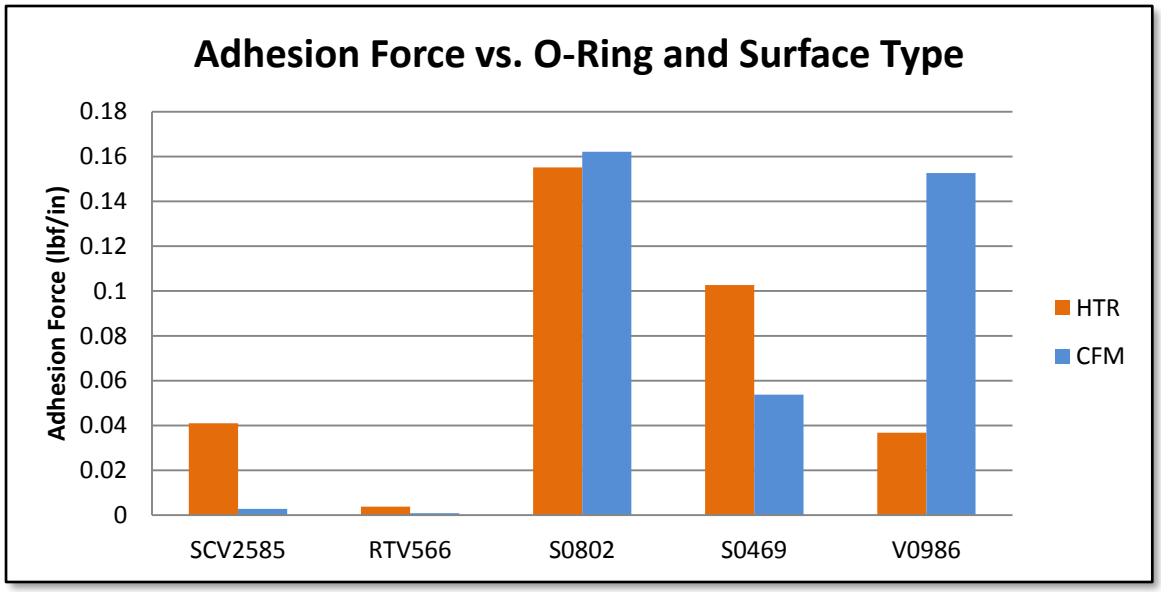

Figure 29: O-Ring Results when Tested with Both HTR and CFM

A similar situation occurred when testing S0899 on N615. This was tested as another program at LL is using this combination for an O-ring and interface. Even though V0986's adhesion force decreased only 0.0245 lbf when applied to N615 versus CFM, S0899's adhesion force decreased by 0.0733 lbf and resulted in almost zero adhesion, as shown in Figure 30. These results suggest that further investigation of O-rings and their adhering interfaces should be done to find low adhesion combinations.

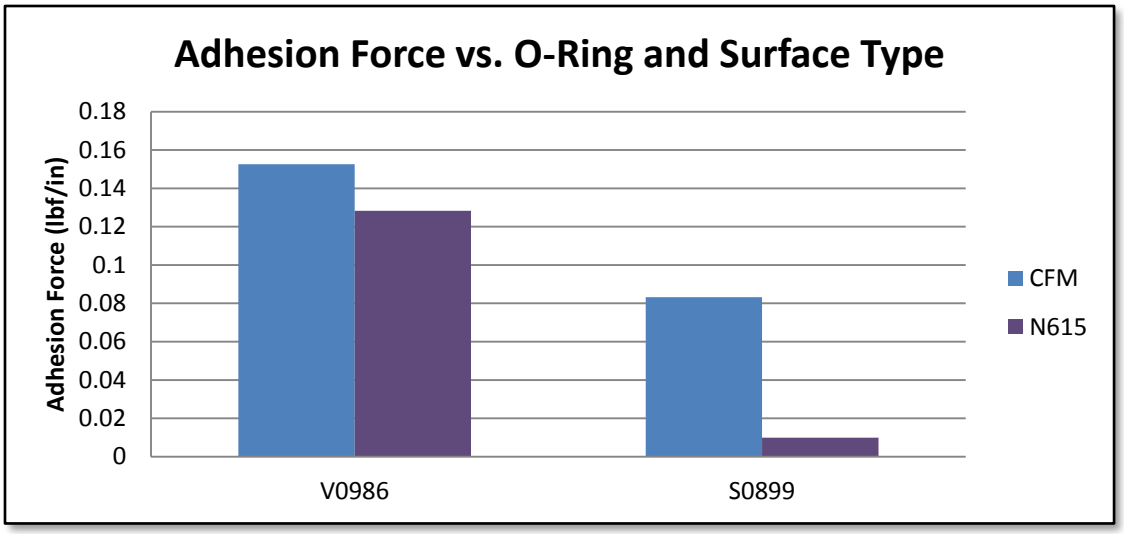

Figure 30: O-Ring Results when Tested with Both N615 and CFM

4.6 Residue/Squish Test Results

The squish test for pre and post bake resulted in very little variance of residue thickness, as shown in Figure 31. All O-rings were within 5 nm of residue for pre and post-bake with the exception of C0267, LM151, and S7440.

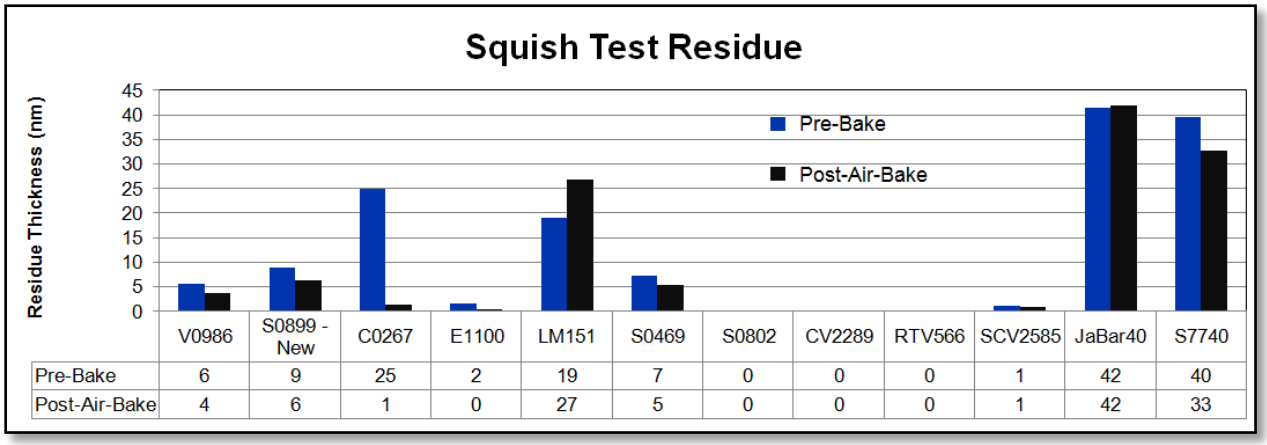

	V0986	S0899 - New	C0267	E1100	LM151	S0469	S0802	CV2289	RTV566	SCV2585	JaBar40	S7740
Pre-Bake	6	9	25	2	19	7	0	0	0	1	42	40
Post-Air-Bake	4	6	1	0	27	5	0	0	0	1	42	33

Figure 31: Squish Test Residue Results

The residue thickness was compared to adhesion, to see if the proposed theory that greater residue correlates to greater adhesion. After plotting and review, no correlation was determined between residue and adhesion, as shown in Figure 32.

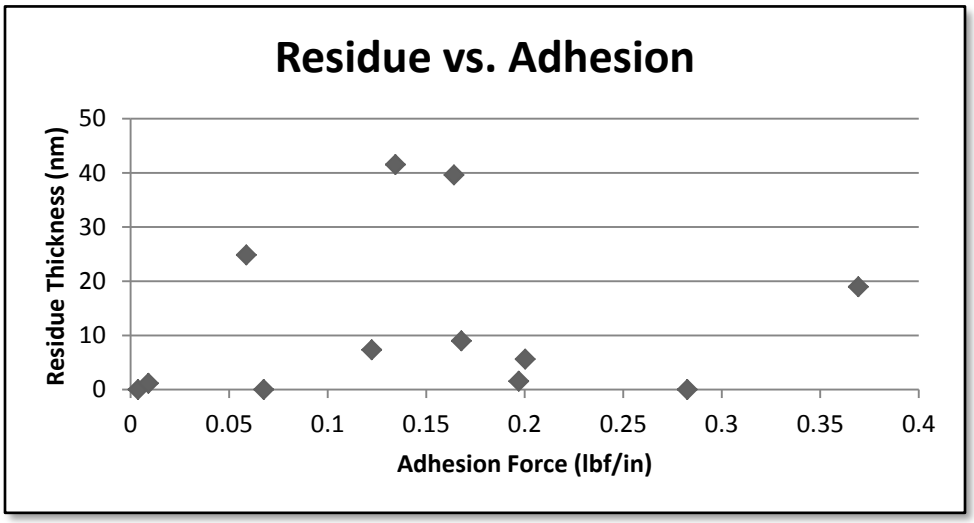

Figure 32: Residue vs. Adhesion Results

4.7 DMA Temperature Testing Analysis

DMA temperature testing was completed on only the final contesting O-rings, of which were S0469, S0899 batch 2 vacuum baked, and SCV2585 vacuum baked. Each of these O-rings yielded low adhesion and stiffness values, as well as passing outgassing standards (with the exception of S0469, see outgassing results), and thermal testing.

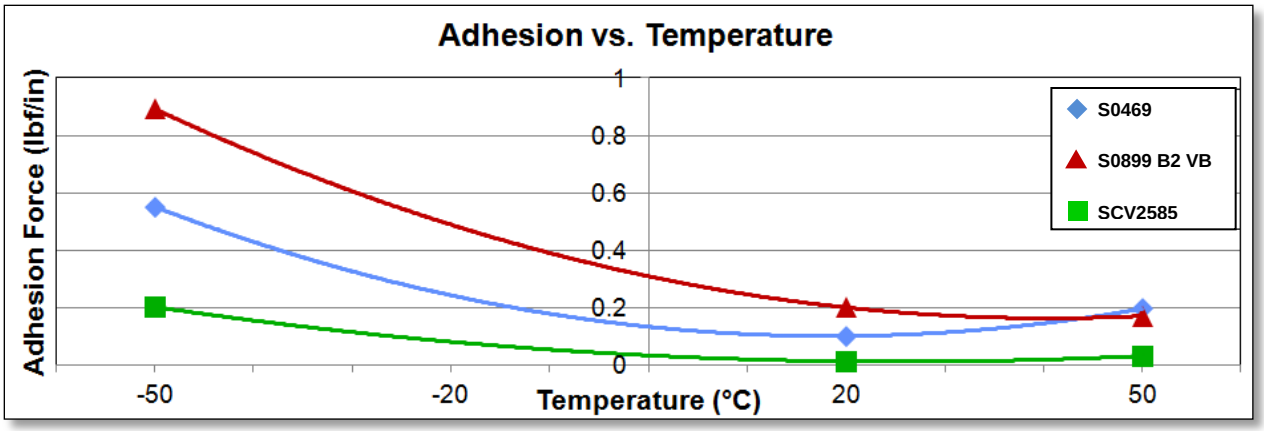

Figure 33: Adhesion vs. Temperature Results for Selected O-Rings

Thermal testing allowed for a large distinction to be made between the different O-rings. All of the O-rings tested relatively well under hot conditions, but their adhesion greatly increased at cold temperatures, fitting the initial hypothesis. As shown in Figure 33, SCV2585 performed the best, and resulted in an average adhesion force of 0.2 lbf/in.

4.8 Overall O-Ring Testing Results

The final O-ring and interface pairing was chosen to be SCV2585 and CFM. Though SCV2585 may perform better on other interfaces other than CFM, more testing must be accomplished to determine the best pairing interface. We are confident that SCV2585 can perform well on CFM, and make our decision a successful one for the ST program.

Chapter 5: Launch Latch Final Analysis and Component Selection

With the choice of SCV2585 as the final O-ring, the analysis of the Launch Latch system was conducted. The average adhesion force for SCV2585 at -50 °C was calculated at the 95% confidence level, and then multiplied by the safety factor of 1.25 and the length of the O-ring (14.7 inches), resulting in an adhesion force of 3.7 lbf. Based on the required force to open the Launch Latch and predetermined upper Vlier spring values determined by the vendors, upper Vlier springs of 4.5 lbf were chosen. The upper Vlier springs were provided by the company Vlier, with the part number SSS48. The remaining specifications for this spring can be found in Appendix F. The lower torsion springs were given as 5 lbf/inch. This adhesion force was then input into MathCAD, along with values for the lower torsion spring and upper Vlier spring values. The sum of the moments in the system when the latch is opening resulted in an overall opening force 2.849 lbf as shown in Figure 34.

$$F_{adhesion} = 3.7\,lbf$$

$$\frac{\left(2M_{LT} + 2F_{vtop}\cdot r_3 - P_z\cdot r_5\right)}{r_1} - F_{adhesion} = 2.849\cdot lbf$$

Figure 34: Overall Opening Force

The O-ring compression force was calculated to be 27 lbf, based on the normalized stiffness of SCV2585 vacuum baked, the O-ring circumference, and the O-ring compression distance of 0.010 inches. The HOPA force with all internal forces of the springs, O-ring compression, etc, accounted for was calculated as 51.9 lbf per HOPA. This force was added to the preload force and dynamic force exerted on the Pawl Arm to find the total force applied to the Pawl Arm, which was determined to be 360.9 lbf. This force was entered into SolidWorks to calculate the

maximum stress on the system which was 87.8 ksi, well below the maximum allowable yield stress of 120 ksi for the system.

The HOPAs were also examined to make sure the force exerted on the shafts would not exceed allowable values. Given by the data sheet, which can be found in Appendix F, the HOPA shafts can withstand 260 lbf of dynamic force and 350 lbf of static force per HOPA. The minimum force the HOPAs can stand was then applied to the safety factor of 1.25, resulting in a maximum shear force of 208 lbf. The total applied HOPA force of 360.9 lbf, when divided between the two HOPAs, results in an applied shear force of 180.5 lbf per HOPA. This applied force is lower than the maximum allowable shear force, making the result viable.

Chapter 6: Conclusions and Recommendations

In this chapter, the overall themes and results of the data are discussed, and recommendations for further O-ring testing are made. O-Ring adhesion is examined, as well as interface adhesion factors, and overall recommendations for further research.

6.1 Factors in O-Ring Adhesion

The main factors that affected O-ring adhesion were the chemical composition of the O-ring/coating, whether the O-ring was vacuum baked or not, and the temperature at which the O-ring was tested. The spread of O-ring adhesion values varied greatly, from a maximum average value of almost 0.5 lbf/inch to a minimum of almost zero, or 0.001lbf/inch. This variance may be explained by an inquiry into the chemical compositions of the O-ring types to better understand their adhesion properties and to make informed choices on O-ring treatments/pairings.

The complexities of O-ring adhesion were exemplified throughout the testing in this project. O-Rings were found to vary greatly in their adhesion due to many factors, some which were observable, and others which were from unknown sources. The unknown sources were theorized to be chemically related, or related to the curing process of the O-ring. Our investigation revealed a large data spread for each type of O-ring, which resulted in the need for further testing. To further explore the complexities of O-rings, more O-rings of similar types (silicone, fluorocarbon, EPDM, etc.) should be explored to see if trends in O-ring adhesion, residue or other parameters exist.

When running the calibration of the DMA, it was identified that if the rate of force was reduced from 5 N/min to 0.25 N/min the calculated force value to lift the top plate with no O-ring became closer to the true value of the weight of the top plate. It is recommended that for further testing, the ramp rate be slowed to collect more accurate data, and therefore fewer data points must be collected.

Due to the data that was retrieved by the S0899 B2 Soak experiment, the use of isopropyl alcohol to clean the O-rings should be limited, and specifically avoid all immersions. O-Rings are very easily affected by secondary chemical use, and although most data sheets suggest that isopropyl alcohol should have little to no effect on O-rings, it may have played a role in O-ring adhesion, as exemplified by our test ("Parker O-Ring Handbook", 1999). Other chemicals to treat the O-rings or the use of no chemical at all should be explored. For O-rings with coatings, such as Parkerslick, it is possible that isopropyl alcohol could have affected the outer coating and therefore the effectiveness of Parkerslick. It is recommended that Parkerslick be tested with no isopropyl wipe to ensure the coating is not affected.

It is also recommended that other plastic-based surface treatments other than FEP coatings are tested on O-rings. Though Teflon is known for its non-stick properties, the FEP encapsulation resulted in very high stiffness values, making them unusable for the Launch Latch. Possibly a thinner film plastic may have little to no adhesion, and be more consistent than an O-ring with no coating in terms of adhesion. Parker provided several other coatings other than Parkerslick, trying other coatings provided by Parker may result in a low adhesion coating.

Due to O-ring vulnerability, for further testing it is recommended that a testing device which does not alter the O-ring from its original shape, or O-rings large enough that sections could be

seen as almost nearly straight, be used. By straightening a curved O-ring, stresses are induced into the O-ring, and the topographical/surface properties of the O-ring changed when compared to its naturally curved shape.

It is also recommended that the O-rings complete life cycle, from formation and curing, to final testing, is recorded when performing O-ring adhesion tests. The chemical properties and physical attributes of O-rings change greatly depending on the way the O-ring is stored and how long it is stored for. It is important to keep track of this information when understanding why various O-rings may perform better or worse.

The simplest solution is to avoid O-rings all-together. If a proper replacement for O-rings can be found that results in little force being applied to the Launch Latch, it would be a worthwhile area to explore.

6.2 Factors in Interface Adhesion

The adhesion of O-rings to a specific interface was not consistent throughout the tests. It is speculated that this is due to chemical interactions between the mating interfaces' surface and the O-ring. Developing a better understanding of the chemical relations between the interfaces and the O-rings may result in better O-ring/interface parings and a better way of determining O-ring pairs. There were times when cleaning residue that the marks appeared to be more like oxidation than plasticizers left on the interface's surface. Some O-rings are capable of releasing oxygen when compressed, which would suggest oxidation as a possible byproduct. The surface treatment of THF is also questionable, though most surfaces should not react with it; there was no information as to its possible interaction with O-rings if any residue from THF remained on the interfaces surface. This should be explored along with isopropyl's effect on O-ring adhesion. The

outgassing of the interfaces should be explored as well to ensure that they cannot deposit any form of residue on the Launch Latch lens.

It was also speculated that differences in O-ring adhesion to one interface may be due to varying surface roughness or coating thickness between similar sample types. It is recommended that surfaces with extreme thin-film coatings, such as a graphite carbon nanotube layer about one molecule thick be applied to a surface. In this case, the O-ring would not be in direct contact with the interface itself, but with the very thin film of graphite. If a type of material which produces low to no adhesion, such as Teflon, was able to be applied to an interface such that O-rings could not adhere to it, then the factor of adhesion itself and its uncertainty is miniscule.

6.3 Possibilities for Future Research

For further research, each type of O-ring should be tested with each interface in order to find the best interface type per O-ring. As demonstrated by the data, not all O-rings perform best with the same surface, therefore adhesion values for one particular type of O-ring versus all the surfaces is not a reasonable comparison, as some surfaces react differently with different O-ring compositions than others. Non-adhering surfaces should be further explored, as the choice of O-ring becomes negligible if no item may adhere to the surface. Other types of O-rings made of other polymer bases should be explored as well.

From our thermal adhesion testing, we concluded the adhesion force of O-rings will increase as temperature decreases. Further testing is needed to confirm our results and look into how exactly this adhesion force increases with temperature. Thermal testing at various temperatures such as -20 °C, 0 °C and any values in-between would help to understand the trend an O-ring's adhesion

has as temperature is decreased. In the end, an equation could possibly be formulated to calculate an O-ring's adhesion force at a given temperature after it has gone through preliminary tests.

What causes this enormous increase in adhesion as temperature decrease is also an important aspect to look into. Perhaps investigate if residue or the plasticizers left behind by the O-rings can freeze at the temperatures we are testing at and what the payload would expect. Although there was no correlation between the amount of residue left behind and the adhesion force at room temperature, this may change as temperature decreases and the plasticizers have a chance to get to a level where they will go through a phase change into a solid. An O-ring with less residue may not adhere nearly as much as temperature decreases, as an O-ring with a large amount of residue left behind.

Overall, there is plenty of room to explore the root causes of O-ring adhesion and this project has only scratched the surface of all the possible factors involved.

Work Cited:

1. Department of Defense, Space Simulation and Applications of Space Technology. (2007). *Standard test method for total mass loss and collected volatile condensable materials from outgassing in a vacuum environment* (E595-07). West Conshohocken, PA: ASTM International.

2. Parker Seals. (1999). *Parker O-Ring Handbook.* Cleveland, OH: Parker Hannifin Corporation.

Appendix A: DMA Testing Standards

Brian Walker

DMA Adhesion Tests

I. <u>Goal:</u>

To be able to measure and then compare the adhesion force between a variety of O-Ring types and various mating surfaces in order to determine the best combination of the two; as well as potentially provide insight into what causes this phenomenon.

II. <u>DMA Procedure for Stiction Testing – Hart Fixture</u>

- Go to DMA user interface on the computer

Option 1: Load stiction sequence

- Filename: **RT July11_2012**

Option 2: Manual Configure

- Enter the following information into the appropriate areas:

  Mode: DMA controlled force

  Test: Custom

  Clamp: Compression

  Sample Shape: square disk (t, w)

  Dimensions: 76.2mm, 3.53mm

Under Procedure:

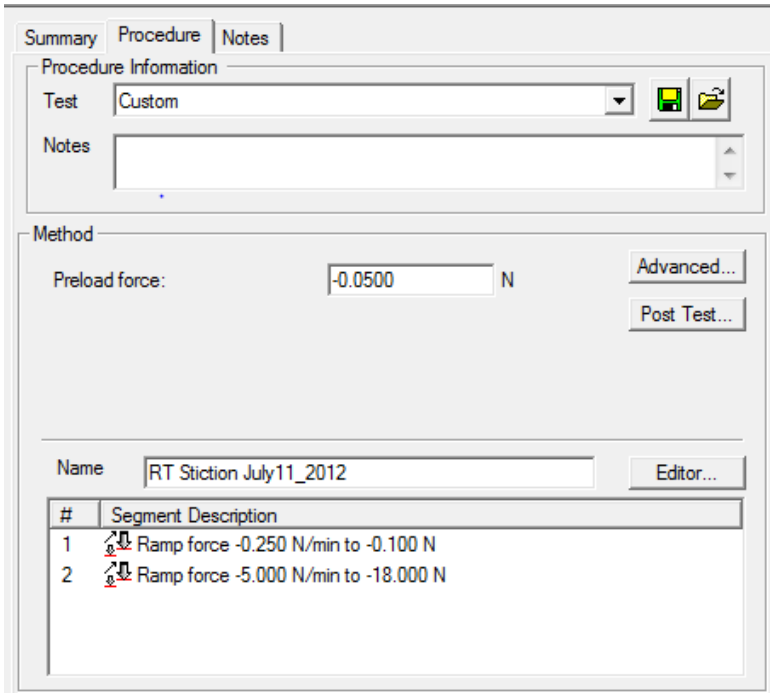

- To change the segment description to match what is seen above, Click on 'Editor…' and then double click on each segment to change the numbers
    - Steps can be added from the column to the right of the segments and can also be deleted if need be

Under Summary:

Sample Name: Components of test sample and date they were assembled

- Ex: *Chemfilmed Mach Al w Viton 6/27*

Comments: Preparation of O-Ring

- Ex: *O-Rings as received but cleaned*

Setup:

- Install the *lower fiber tension* adapter by placing it onto central moving shaft
- Remove cone-shaped cap from adapter and use Allen wrench to tighten adapter onto shaft
- Install the dovetailed, oval test base, making sure to insert the temperature sensor through the clearance hole

- Place 8-32 screws through the four support posts and tighten to secure test base (picture available)
- Slide one of the O-Ring base plates into test base (with no o-ring)

<u>Preparing Central Shaft for Calibration:</u>

- Slide 2 reduced outer diameter ¼-20 washers onto bare adapter and then install aluminum Hart Fixture clamp adapter.
- Thread acorn nut onto aluminum clamp adapter
- Loosely thread ¼-20 nut onto aluminum clamp adapter

<u>Calibration:</u>

- Go to Calibrate->Clamp->make sure *Clamp Type* is 'Compression' and *Calibration Type* is
  'All Calibrations', then hit 'Next'
- Press 'Calibrate' for clamp mass. Ignore open furnace warning
- After mass calibration, hit 'Next'
- Remove ¼-20 nut and install top plate by securing it into position with two 4-40 SHC screws tightly so that there is metal to metal contact
- Lift up on center shaft, so that base plate just lifts off of test base.
  - Eye-ball setup and make sure that when the base plate lifts off, it is parallel to the test base
- After determining lift-off was parallel, with partner holding the fixture in place, tighten the L-shaped brackets on either side of the base plate, **MAKING SURE NOT TO ALLOW FIXTURE TO SHIFT AT ALL. IF IT DOES SHIFT, LOOSEN BRACKETS AND START AGAIN.**
- Install nut onto Hart fixture so that there is metal-to-metal contact between the top plate and bottom of nut
- Leave G*auge Block Length*=zero
- Hit 'Calibrate' for clamp zero
- When clamp zero calibration is finished, hit 'Next'
- Hit 'Calibrate' for clamp compliance
- Hit 'Next' to view calibration report
- Hit 'Finish'
  You are now calibrated and ready to test.

Calibration Test:

- Under Summary tab, change file name to 'July11-2012_Calibration' (use current date)
- Create a new folder using the correct naming convention for whichever test sample you are testing and put this file under this new folder
    - *Example Folder Name: CFM_V0986_Sx*
- With partner clamping down on top plate with hands, slowly and carefully back off each corner screw, alternating to ensure even lift-off. Remove screws
- Hit 'Run'
    - Right-click on red graph and click on 'Signals'
    - Change X-Axis 'Signal Name' to Time if need be
- When system is tripped due to the "popping" of the top plate, you may hear the nitrogen tanks start whistling and an alert will appear on the computer screen. Hit the red stop button in the top-right corner of the screen

Analysis:

- Open **TA Universal Analysis** on the desktop
- Click File->Open. Find your newly created folder and open the calibration run.
    - The folder sequence goes as follows:
        - C Drive->TA->Data->DMA->Oring Stiction Initiative Test Data->Corresponding Test folder
- Click on 'Signals' and make sure Y1 is *Static Force* and all other Y's are *Not Used*. and X is *Time*
    - Save these settings and then hit 'OK'
- Verify the *Parameters* match what you want and then click 'OK'
- Right-click on the very end of the plot and select 'Label Point'
    - Make sure it will be labeled with 'Time' and 'Y-Axis'
- Hit 'OK'
- Click on the button with an 'A' at the end of a pencil
- In this text box, enter the weight of the top plate, the calculated stiction force, and visual observations as they pertain to residue left behind (not necessary for calibration)

    - For samples with visible residue, take at least one picture per sample-component set and upload using Carl's camera. Save under appropriate folder
    - Verify that the stiction force for the test run is <.01 N or thereabout
- Go to File->Export PDF. Make sure you are under the correct folder and save the file
- Go to File->Save Session. Save the session under the correct folder with the same name
    - Ex: *CFM_JABAR40_Sx*

<u>Sample Tests:</u>

- Remove nut and O-Ring fixture, break down set up to test base
- Load test sample into test base and repeat initial setup steps from the calibration test.
    - *(Make sure plate lifts off evenly when you lift up on central shaft, hold in place and tighten L-brackets, prevent any shifting of setup)*
- Screw nut back onto aluminum shaft adapter, again until metal-to-metal contact
- Under Summary tab, change file name to reflect current components 'CFM_V0986_S1'
- Hit 'Run'
    - Right-click on red graph and click on 'Signals'
    - Change X-Axis 'Signal Name' to Time if need be
- When system is tripped due to the "popping" of the top plate, you may hear the nitrogen tanks start whistling and an alert will appear on your computer screen. Hit the red stop button in the top-right corner of the computer screen
- Open **TA Universal Analysis** on the desktop and follow the ***<u>Analysis</u>*** instructions
- Save collected data under Stiction folder using the naming convention INTERFACE_ORINGTYPE_SAMPLE#
    - Ex: **Chemical-Filmed Machined Al on Viton, sample 3** would be **CFM_V0986_S3**
- **Repeat 'Sample Tests' Procedure for all subsequent tests of the same O-Ring and interface types. Make sure to change the Data File name each run to show the correct sample number**

Appendix B: Outgassing Standards

For Entire Work -See CD File: E595 Standards

For reference, see work cited.

Designation: E595 – 07

Standard Test Method for Total Mass Loss and Collected Volatile Condensable Materials from Outgassing in a Vacuum Environment[1]

This standard is issued under the fixed designation E595; the number immediately following the designation indicates the year of original adoption or, in the case of revision, the year of last revision. A number in parentheses indicates the year of last reapproval. A superscript epsilon (ε) indicates an editorial change since the last revision or reapproval.

This standard has been approved for use by agencies of the Department of Defense.

1. Scope

1.1 This test method covers a screening technique to determine volatile content of materials when exposed to a vacuum environment. Two parameters are measured: total mass loss (TML) and collected volatile condensable materials (CVCM). An additional parameter, the amount of water vapor regained (WVR), can also be obtained after completion of exposures and measurements required for TML and CVCM.

1.2 This test method describes the test apparatus and related operating procedures for evaluating the mass loss of materials being subjected to 125°C at less than 7×10^{-3} Pa (5×10^{-5} torr) for 24 h. The overall mass loss can be classified into noncondensables and condensables. The latter are characterized herein as being capable of condensing on a collector at a temperature of 25°C.

NOTE 1—Unless otherwise noted, the tolerance on 25 and 125°C is ±1°C and on 23°C is ±2°C. The tolerance on relative humidity is ±5 %.

1.3 Many types of organic, polymeric, and inorganic materials can be tested. These include polymer potting compounds, foams, elastomers, films, tapes, insulations, shrink tubings, adhesives, coatings, fabrics, tie cords, and lubricants. The materials may be tested in the "as-received" condition or prepared for test by various curing specifications.

1.4 This test method is primarily a screening technique for materials and is not necessarily valid for computing actual contamination on a system or component because of differences in configuration, temperatures, and material processing.

1.5 The criteria used for the acceptance and rejection of materials shall be determined by the user and based upon specific component and system requirements. Historically, TML of 1.00 % and CVCM of 0.10 % have been used as screening levels for rejection of spacecraft materials.

1.6 The use of materials that are deemed acceptable in accordance with this test method does not ensure that the system or component will remain uncontaminated. Therefore, subsequent functional, developmental, and qualification tests should be used, as necessary, to ensure that the material's performance is satisfactory.

1.7 *This standard does not purport to address all of the safety concerns associated with its use. It is the responsibility of the user of this standard to establish appropriate safety and health practices and determine the applicability of regulatory limitations prior to use.*

2. Referenced Documents

2.1 *ASTM Standards:*[2]

E177 Practice for Use of the Terms Precision and Bias in ASTM Test Methods

2.2 *ASTM Adjuncts:*

Micro VCM Detailed Drawings[3]

3. Terminology

3.1 *Definitions:*

3.1.1 *collected volatile condensable material, CVCM*—the quantity of outgassed matter from a test specimen that condenses on a collector maintained at a specific constant temperature for a specified time. CVCM is expressed as a percentage of the initial specimen mass and is calculated from the condensate mass determined from the difference in mass of the collector plate before and after the test.

3.1.2 *total mass loss, TML*—total mass of material outgassed from a specimen that is maintained at a specified constant temperature and operating pressure for a specified time. TML is calculated from the mass of the specimen as measured before and after the test and is expressed as a percentage of the initial specimen mass.

3.1.3 *water vapor regained, WVR*—the mass of the water vapor regained by the specimen after the optional reconditioning step. WVR is calculated from the differences in the specimen mass determined after the test for TML and CVCM

[1] This test method is under the jurisdiction of ASTM Committee E21 on Space Simulation and Applications of Space Technology and is the direct responsibility of Subcommittee E21.05 on Contamination.

Current edition approved Dec. 1, 2007. Published December 2007. Originally approved in 1977. Last previous edition approved in 2006 as E595 – 06. DOI: 10.1520/E0595-07.

[2] For referenced ASTM standards, visit the ASTM website, www.astm.org, or contact ASTM Customer Service at service@astm.org. For Annual Book of ASTM Standards volume information, refer to the standard's Document Summary page on the ASTM website.

[3] Available from ASTM International, 100 Barr Harbor Dr., PO Box C700, West Conshohocken, PA 19428–2959. Order Adjunct ADJE0595.

Copyright. (C) ASTM International, 100 Barr Harbor Drive, PO box C700 West Conshohocken, Pennsylvania 19428-2959, United States

Copyright by ASTM Int'l (all rights reserved); Tue Oct 9 12:06:05 EDT 2012
Downloaded/printed by
MIT Libraries pursuant to License Agreement. No further reproductions authorized.

Appendix C: HOPA Data Sheet

For full SP-5025 Pin Puller Specifications, see attached CD file: SP-5025 Data Sheet and SP-5025 Specification

SP-5025 HOP Actuator

General Description

The Starsys SP-5025 Auto Shut Off Pin Puller contains the same heritage design as the standard EP-5025 pin puller for which it replaces. It includes the added feature of fully redundant internal circuit interrupts which discontinue power to the actuator once full retraction has been reached. This design reduces overall system cost by simplifying control requirements. The SP-5025 may be powered by a single timed power pulse to one of the fully redundant heater circuits. The dual heaters and dual circuit interrupts can be wired by the user to provide for automonous or interactive control system designs.

Features:

- Integral circuit interupts
- Simple control system
- Gentle, High-force retraction
- Resettable without refurbishment
- Non-explosive
- Minimal safety requirements

Specifications

Mechanical	US	SI
Envelope Dimensions	2.42 x 1.48 in	6.147 cm x 3.75 cm
Misalignment Capability	0	
Mass	2.82 oz max	80.0 g max
Life Cycles (Full Stroke)	>500 @ 50 lbf >100 @ 100 lbf	>500 @ 222 N >100 @ 445 N
Redundancy	Heaters, Circuit Interrupts	
Operation Time	360 sec. max	
Source Shock	0	
Stroke	0.310 in	7.87 mm
Output Force	100 lbf min.	444 N min.
Shear Force	350 lbf Quasi-Static 260 lbf Dynamic	1557 N 1154 N
Electrical		
Power Input	22 to 34V DC, 28V Nominal, 15 Watts	
Heater Resistance	52.3 ohms ±5%	
Telemetry	Redundant	
Connectors	Flying Leads	
Thermal		
Operating Temperatures	-85° to +176° F	-65° to +80° C
Non-Operating Temperatures	-319° to +176° F	-195° to +80° C
Reset Tools Needed	Manual Reset Tool EP-7032 Pneumatic Tool EP-7056	
Reset Time	<10 minutes	
Access	See ICD	

Data for information only and subject to change. Contact Starsys for design data.

STARSYS RESEARCH

19

4909 Nautilus Ct. North • Boulder, CO 80301 USA • voice: 303-530-1925 • fax: 303-530-2401•www.starsys.com

Appendix D: Surface Coating Specifications

All materials below were provided by LL Staff:

==========

SANFORD QUANTUM/HARDLUBE (ALUMINUM ONLY)

2. FINISH: PART TO BE TREATED WITH THE FOLLOWING SEQUENCE:

2.A CHEMICAL FILM ENTIRE PART PER MIL-DTL-5541.

2.B MASK ALL AREAS, INCLUDING ALL THREADED HOLES, THAT WILL NOT RECEIVE THE SANFORD PROCESS TREATMENT.

2.C SANFORD QUANTUM HARDCOAT.

2.D NICKEL ACETATE SEAL.

2.E SANFORD HARDLUBE.

NOTE: TOTAL COATING TO BE .002 INCHES (.001 IN PENETRATION, .001 IN BUILD UP). CURE TEMPERATURES SHALL NOT EXCEED +200 DEG C (+392 DEG F) TO PREVENT ANNEALING OF THE BASE METAL.

BY SANFORD PROCESS CORPORATION

1 SHORR COURT

WOONSOCKET, RI, 02895

PHONE: 401-597-5000

==========

NEDOX NH-1 (ALUMINUM)

2. FINISH: PART TO BE TREATED WITH THE FOLLOWING SEQUENCE:

2.A MASK ALL AREAS, INCLUDING ALL THREADED HOLES, THAT WILL NOT RECEIVE THE NH-1 PROCESS TREATMENT.

2.B NEDOX NH-1, COATING THICKNESS .0008-.0012 PER SURFACE. CURE TEMPERATURES SHALL NOT EXCEED +200 DEG C (+392 DEG F) TO PREVENT ANNEALING OF THE BASE METAL.

2.C MASK ALL NEDOX COATED AREAS.

2.D CHEMICAL FILM ENTIRE PART PER MIL-DTL-5541.

BY GENERAL MAGNAPLATE

1331 ROUTE 1

LINDEN, NJ 07036

PHONE: 908-862-6200

==========

DICRONITE (ALUM)

2. FINISH: PART TO BE TREATED WITH THE FOLLOWING SEQUENCE:

2.A CHEMICAL FILM ENTIRE PART PER MIL-DTL-5541

2.B MASK ALL AREAS, INCLUDING ALL THREADED HOLES,THAT WILL NOT RECEIVE THE DICRONITE PROCESS TREATMENT.

2.C DICRONITE COAT. MAXIMUM COATING TO BE 20 MICRO-INCHES (0.5 MICRONS). CURE TEMPERATURES SHALL NOT EXCEED +200 DEG C (+392 DEG F) TO PREVENT ANNEALING OF THE BASE METAL.

BY DICRONITE

66 MAINLINE DRIVE

WESTFIELD, MA 01085

PHONE: 413-562-5019

==========

DICRONITE (INVAR 36)

2. FINISH: PART TO BE TREATED WITH THE FOLLOWING SEQUENCE:

2.A MASK ALL AREAS, INCLUDING ALL THREADED HOLES,THAT WILL NOT RECEIVE THE DICRONITE PROCESS TREATMENT.

2.B DICRONITE COAT. MAXIMUM COATING TO BE 20 MICRO-INCHES (0.5 MICRONS). CURE TEMPERATURES SHALL NOT EXCEED +200 DEG C (+392 DEG F) TO PREVENT ANNEALING OF THE BASE METAL.

BY DICRONITE

66 MAINLINE DRIVE

WESTFIELD, MA 01085

PHONE: 413-562-5019

==========

TUFRAM L-4 (ALUM) HTR

4. DESIGNATED SURFACE TO BE TREATED WITH TUFRAM L-4.

COATING THICKNESS .001 PER SURFACE.

CURE TEMPERATURES SHALL NOT EXCEED +200 DEG C (+392 DEG F)

TO PREVENT ANNEALING OF THE BASE METAL.

BY GENERAL MAGNAPLATE

1331 ROUTE 1

LINDEN, NJ 07036

PHONE: 908-862-6200

==========

NEDOX SF-2 (INVAR ONLY)

4. FINISH: TBD

BY GENERAL MAGNAPLATE

1331 ROUTE 1

LINDEN, NJ 07036

PHONE: 908-862-6200

==========

NEDOX 615, WHITE (INVAR ONLY)

2. FINISH: PART TO BE TREATED WITH THE FOLLOWING SEQUENCE:

2.A MASK ALL AREAS, INCLUDING ALL THREADED HOLES,THAT WILL NOT RECEIVE THE NEDOX PROCESS TREATMENT.

2.B DESIGNATED SURFACE TO BE TREATED WITH NEDOX 615, WHITE. CURE TEMPERATURES SHALL NOT EXCEED +371 DEG C

(+700 DEG F) TO PREVENT DEGRADING INVAR PROPERTIES.

BY GENERAL MAGNAPLATE

1331 ROUTE 1

LINDEN, NJ 07036

PHONE: 908-862-6200

For Bead Blasted or Polished Finishes (work by Brian Walker)

Surface Roughness Experimentation Procedure:

In order to test the effects of surface roughness on stiction force, we will use three different finishes on our standard aluminum top plates: as-received machine finish, polished, and sand-blasted. All will be chemical-filmed and precision cleaned before the stiction tests are run.

To prepare the baseline, as-received machined plates, we will just use the top plates without any special finish process. We would look at each individual top plate and select the side that would come into contact with the O-Ring based on which side looked to be smoother and had less noticeable machining grooves.

The sand-blasted top plates required a sand-blasting finish (obviously) which was performed by Technician Roger Shields in the Polymer Lab. In an attempt to standardize our roughness levels, all pieces were blasted using Number 8 grit with an operating pressure of 60 psi. To determine which blasting procedure would work best, we sectioned off a 6” x 18” piece of aluminum stock and varied the working distance and number of passes with the blaster. What we settled upon was a working distance of 3-4” and 4 total passes for each surface. The pieces were rotated 90° counterclockwise between each pass. The trajectory of the shot was approximately perpendicular

to the plate surface. Both sides were blasted to allow for twice as many tests. After all passes were completed, each piece was carefully wiped down with isopropanol, dried, chemical-filmed, and sent to be precision cleaned. Although blasting is a process that is almost impossible to repeat perfectly, we will still be able to yield results that will show whether there is a correlation between stiction force and surface roughness of the substrate.

The polished top plates were prepared by Mike Walsh in the polishing lab. The parts were first lapped with 3 micron alumina grit on glass for about 2.5 hours. Next they were polished with 0.5 micron Hastilite Polytron. This polish is a solution containing 0.5 micron diamond. This polishing step was performed on a SUBA 500 polishing pad and lasted about 4 hours.

This experiment will be completed using the V0896-50 Viton O-Ring sample and the plates will be clamped down for 2 weeks. There will be a total of 15 samples being tested: 5 for each roughness level. 15 mil shim stock will be placed in between the top and base plates for standardized spacing. All preparations will be performed in clean-room I-209. Before any samples are prepared, all top plates will be tested on the Zygo NV 5000 to catalogue their mean surface roughness, surface roughness depth, and Rms roughness. Conclusions will be drawn when samples are measured on the DMA. This equipment will ultimately tell us the force required to separate the plates, thus the stiction force.

Appendix E: O-Ring Specification Sheets

Compound Data Sheet
Parker O-Ring Division United States

MATERIAL REPORT

REPORT NUMBER: KA1058A
DATE: 09/26/91

TITLE: Evaluation of Parker Compound C0267-50 to specification MIL-R-3065C, ASTM D 2000 2BC 515 A14 E014 EO34.

PURPOSE: To show compliance of all phases of specification.

CONCLUSION: Parker Compound meets or exceeds all phases of the specification above.

Recommended temperature limits: -60°F to 250°F

Recommended For
Carbon Dioxide
Ammonia
Refrigerants
Silicone oil and grease
Water and water solvents at low temperatures

Not Recommended For
Aromatic hydrocarbons, e.g, benzene
Chlorinated hydrocarbons
Polar solvents, e.g. ketones, esters, ethers, acetones

Parker O-Ring Division
2360 Palumbo Drive
Lexington, Kentucky 40509
(859) 269-2351

Compound Data Sheet
Parker O-Ring Division United States

MATERIAL REPORT

TITLE: Evaluation of Parker Compound E1100-50 when immersed in water glycol solution.

PURPOSE: To obtain general data for E1100-50.

Recommended temperature limits: -70°F to 250 °F

Recommended For
Hot water and steam
Glycol based brake fluid
Many organic and inorganic acids
Cleaning agents, soda and potassium alkalis
Phosphate –ester based hydraulic fluids
Silicone oil and grease
Polar solvents
Ozone, Aging and weather resistance

Not Recommended For
Mineral oil products

Parker O-Ring Division
2360 Palumbo Drive
Lexington, Kentucky 40509
(859) 269-2351

Compound Data Sheet
Parker O-Ring Division United States

MATERIAL REPORT

DATE: 3/8/2002

TITLE: Evaluation of LM151-50 to (formerly 11645).

PURPOSE: To obtain general data for LM151-50 (11645)

Recommended temperature limits: -100 °F to 350 °F

Recommended For
Aromatic mineral oils (IRM 903 oil)
Petroleum oils
Low molecular weight automatic hydrocarbons (benzene, toluene)
Jet Fuels
Chlorinated Solvents
Dry heat and low temp

Not Recommended For
Phosphate-esters
Acids
Ketones
Amines (ammonia)
Auto and aircraft brake fluids

Parker O-Ring Division
2360 Palumbo Drive
Lexington, Kentucky 40509
(859) 269-2351

Compound Data Sheet
Parker O-Ring Division United States

MATERIAL REPORT

REPORT NUMBER: KK1556
DATE: 02/09/83

TITLE: Evaluation of Parker Compound S0469-40 to AMS 3301E Specifications

PURPOSE: To determine if S0469-40 meets the requirements.

CONCLUSION: Compound S0469-40 meets the requirements.

Recommended temperature limits: -75^{0}F to 400^{0}F

Recommended For
Dry heat
Some petroleum oils
Moderate water resistance
Fire resistant hydraulic fluids (HFD-R and HFD-S)
Ozone, aging, and weather resistance
Low temperature

Not Recommended For
Ketones
Acids
Silicone oils
Auto and aircraft brake fluid

Parker O-Ring Division
2360 Palumbo Drive
Lexington, Kentucky 40509
(859) 269-2351

Compound Data Sheet
Parker O-Ring Division United States

MATERIAL REPORT

REPORT NUMBER: KK2190
DATE: 04/06/93

TITLE: Evaluation of Parker Compound S0802-40 to ASTM D2000 M2GE405 A19 B37 EA14 E016 F19

PURPOSE: To determine if S0802-40 meets the callout.

CONCLUSION: Compound S0802-40 meets the ASTM D2000 callout.

Recommended temperature limits: -60^0F to 400^0F

Recommended For
Dry heat
Some petroleum oils
Moderate water resistance
Fire resistant hydraulic fluids (HFD-R and HFD-S)
Ozone, aging, and weather resistance
Low temperature

Not Recommended For
Ketones
Acids
Silicone oils
Auto and aircraft brake fluid

Parker O-Ring Division
2360 Palumbo Drive
Lexington, Kentucky 40509
(859) 269-2351

Compound Data Sheet
Parker O-Ring Division United States

MATERIAL REPORT

REPORT NUMBER: KB4403
DATE: 06/01/84

TITLE: Evaluation of Parker Compound S0899-50 to ZZ-R-765B, Class 1a and 1b, Grade 50 Specifications

PURPOSE: To determine if S0899-50 meets the callout.

CONCLUSION: Compound S0899-50 meets the requirements.

Recommended temperature limits: -103^{0}F to 400^{0}F

Recommended For
Dry heat
Some petroleum oils
Moderate water resistance
Fire resistant hydraulic fluids (HFD-R and HFD-S)
Ozone, aging, and weather resistance
Low temperature

Not Recommended For
Ketones
Acids
Silicone oils
Auto and aircraft brake fluid

Parker O-Ring Division
2360 Palumbo Drive
Lexington, Kentucky 40509
(859) 269-2351

Compound Data Sheet
Parker O-Ring Division United States

MATERIAL REPORT

REPORT NUMBER: KK1542
DATE: 12/09/82

TITLE: Evaluation of Parker Compound V0986-50

PURPOSE: To obtain general information

Recommended temperature limits: -15^{0}F to 400^{0}F

Recommended For

Petroleum, mineral, and vegetable oils
Silicone fluids
Aromatic hydrocarbons (benzene, toluene)
Chlorinated hydrocarbons
High vacuum
Ozone, weather, aging resistance

Not Recommended For
Hot water and steam
Auto and aircraft brake fluids
Amines
Ketones
Low molecular weight esters and ethers

Parker O-Ring Division
2360 Palumbo Drive
Lexington, Kentucky 40509
(859) 269-2351

Product Profile

NuSil SILICONE TECHNOLOGY

Creative Partners in a Material World

NuSil Technology LLC
[illegible]
[illegible]
[illegible]
An ISO 9001 and AS9100 Certified Company

CV-2289-1

Controlled Volatility Potting and Encapsulating Silicone Elastomer

Description

- Two-part, white silicone system
- Offers a high tear strength, good physical properties and a broad operating temperature range
- Convenient 1:1 mix ratio (Part A: Part B)

Meets or exceeds the ASTM E 595 low outgas specifications outlined in NASA SP-R-0022A and European Space Agency PSS-014-702, with a TML of ≤1% and CVCM of ≤0.1%

Applications

- For applications requiring low outgassing and minimal volatile condensables under extreme operating conditions
- To provide protection of electric components and assemblies against shock, vibration, moisture, dust, chemicals and other environmental hazards
- Ideal for use in potting connectors, cable harness breakouts, molded high-voltage terminals, seals and gaskets due to its high tear strength
- For use as an adhesive
- For applications requiring a broader operating temperature range

Properties	Average Result	ASTM	NT-TM
Uncured:			
Appearance*	White	D2090	002
Viscosity, Part A*	60,000 cP (60,000 mPas)	D1084, D2196	001
Viscosity, Part B*	40,000 cP (40,000 mPas)	D1084, D2196	001
Work Time*	30 minutes	-	008
Tack-Free Time*	4 hours	C679	005
Cured: 15 minutes @ 150°C (302°F)			
Durometer, Type A*	30	D2240	006
Tensile Strength*	700 psi (4.8 MPa)	D412	007
Elongation*	350%	D412	007
Lap Shear Strength* (primed w/ CF1-135)	400 psi (2.8 MPa)	D1002	010
Young's Modulus	325 psi (2.2 MPa)	-	-
Coefficient of Linear Thermal Expansion			
Below Tg (-150°C to -115°C)	60 ppm/°C (60 µm/m/°C)	D3386	-
Above Tg (-95°C to 250°C)	445 ppm/°C (445 µm/m/°C)	D3386	-
Dielectric Strength	955 volts/mil (37.6 kV/mm)	D149	-
Thermal Conductivity	0.230 W/(mK) (55×10^{-5} cal/(cm-sec-°C))	E1530	101
Dynamic Mechanical Analysis (DMA)	See Attached Graph	D4065	-
Collected Volatile Condensable Material (CVCM)*	0.04%	E 595	072
Total Mass Loss (TML)*	0.44%	E 595	072

*Properties tested on a lot-to-lot basis. Do not use the properties shown in this technical profile as a basis for preparing specifications. Please contact NuSil Technology for assistance and recommendations in establishing particular specifications.

Product Profile

NuSil SILICONE TECHNOLOGY

Creative Partners in a Material World

NuSil Technology LLC
[illegible]
[illegible]
[illegible]
An ISO 9001 and AS9100 Certified Company

SCV-2585

Ultra Low Outgassing™ Potting and Encapsulating Silicone Elastomer

Description

- Two-part, translucent silicone system
- Offers a high tear strength, good physical properties and a broad operating temperature range
- Convenient 1:1 mix ratio (Part A:Part B)

Exceeds the ASTM E 595 low outgas specifications outlined in NASA SP-R-0022A and European Space Agency PSS-014-702, with a TML of ≤0.1% and CVCM of ≤0.010%

Applications

- For electronic and space applications requiring *Ultra Low Outgassing™* and minimal volatile condensables under extreme operating conditions
- To provide protection of electronic components and assemblies against shock, vibration, moisture, dust, chemicals and other environmental hazards
- Ideal for use in potting connectors, cable harness breakouts, molded high-voltage terminals, seals and gaskets due to its high tear strength
- For applications requiring a broader operating temperature range

Properties	Average Result	ASTM	NT-TM
Uncured:			
Appearance	Translucent	D2090	002
Work Time	1 hour	-	008
Viscosity, Part A	56,000 cP (56,000 mPas)	D1084, D2196	001
Viscosity, Part B	43,000 cP (43,000 mPas)	D1084, D2196	001
Cured: 15 minutes @ 150°C (302°F)			
Durometer, Type A	35	D2240	006
Tensile Strength	700 psi (4.8 MPa)	D412	007
Elongation	300%	D412	007
Tear Strength	40 ppi (7.1 kN/m)	D624	009
Lap Shear Strength (primed w/ CF1-135)	475 psi (3.3 MPa)	D1002	010
Collected Volatile Condensable Material (CVCM)	0.007%	E 595	072
Total Mass Loss (TML)	0.08%	E 595	072

Properties tested on a lot-to-lot basis. Do not use the properties shown in this technical profile as a basis for preparing specifications. Please contact NuSil Technology for assistance and recommendations in establishing particular specifications.

Instructions for Use

Mixing
Mix Part A and B in a 1:1 mix ratio. SCV-2585 is ideal for Static mix and dispense application.

Vacuum Deaeration
Remove air entrapped during mixing by common vacuum deaeration procedure, observing all applicable safety precautions. Slowly apply full vacuum to a container rated for use and at least four times the volume of the material being deaerated. Hold vacuum until bulk deaeration is complete.

Substrate Considerations
Cures in contact with most materials common to electronic assembles. Exceptions include butyl and chlorinated rubbers, some RTV silicones and unreacted residues of some curing agents. Units being encapsulated or potted should be clean and free of surface contaminates. Containers and dispensers being used should also be clean and dry. Cure inhibition can usually be prevented by washing all containers with solvent or volatizing the contaminant by heating.

Packaging

50 Gram Kit
500 Gram Kit

Warranty

6 Months

ParkerSlick Coating

Alternative Seal Coating with Added Benefits

Customer Value Proposition:

Parker offers an alternative to standard polytetrafluoroethylene (PTFE) coatings called ParkerSlick. ParkerSlick is an external o-ring coating that provides excellent adhesion and friction properties over PTFE. It is dry to the touch, does not rub off easily and unlike PTFE, does not leave any visible residue behind. ParkerSlick comes in an array of colors and offers many significant benefits as listed below.

Contact Information:

Parker Hannifin Corporation
O-Ring Division
2360 Palumbo Dr.
Lexington, KY 40509

phone 859 269 2351
fax 859 335 5128

www.parker.com

Benefits:

- Reduce friction for ease of installation
- May reduce running friction in some dynamic applications where traditional PTFE would not be recommended
- Contrasting colors eliminate in-plant errors

Recommended For:

- Static radial applications where sealing fluids
- Some dynamic applications
- Color identification aid

Parker

ENGINEERING **YOUR** SUCCESS.

Appendix F: Vlier Spring Specifications

HOME | CUSTOMER SERVICE | REQUEST QUOTE | INDUSTRIES & APPLICATIONS | ABOUT VLIER

Proud to be ISO 9001 Certified

SEARCH THE SITE:

PRODUCT MENU

SPRING LOADED DEVICES

- Standard Plungers
- Stubby Plungers
- Ball Plungers
- Push-Fit Plungers
- Ball Buttons & Vlier Wrench
- Quick Release Devices
- Leveling Devices
- Mechanical Components
- RoHS Compliant Products

Find a Local Distributor

COMPETITOR PART NO. CROSS REFERENCE

Visit Our CAD Library

Cage Code 01226

Distributor Log In

STANDARD PLUNGERS - Steel & Stainless Steel

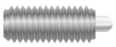

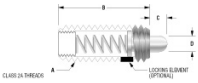

Vlier standard plungers offer long travel, large bearing surfaces and numerous material and design options.

Typical Uses

- Positioning
- Detents
- Indexes
- Ejecting
- Contacts
- Lifters
- Locking
- Insulators
- Latches

Special Features

- Easy Installation
- Corrosion resistance
- Heavy & light end forces
- Self-lubricating materials
- Accurate alignment
- Non-marring materials
- Wear resistance
- Non-chipping materials
- Special environments
- Insulating properties

Standard Plungers - Steel/Stainless Steel

Part No.		End Force, Lbs.			A	B	C	D
Steel	Stainless Steel	Init.	Mid.	Final				
S48	SSS48	1.5	3.0	4.5	6-32	17/32	1/16	.044-.045

Appendix G: CD Files and References

For collected adhesion data, see CD file:Stiction Test Summary – Oct 9

For collected force vs. deflection data, see CD file: Force Vs. Deflection Data

For surface roughness measurements, see CD file: Roughness Measurements

For HOPA specifications, see CD file: SP-5025 Data Sheet & SP-5025 Specification

For MQP the overview/problem statement, see CD file: MQP Summary v4

For FEM SolidWorks file, see CD file: FEA Analysis Pawl Arm

For MathCAD file, see CD file: MQP Calculations FBD